CHAPTER 5

Landau Damping

As the previous chapters demonstrated, there are a large number of collective instability mechanisms acting on a high intensity beam in an accelerator, demanding a wide range of (sometimes conflicting) stability conditions. Yet the beam as a whole seems basically stable, as evidenced by the existence of a wide variety of working accelerators, many of them with demanding beam intensities. One of the reasons for this fortunate outcome is *Landau damping*,[1] which provides a natural stabilizing mechanism against collective instabilities if particles in the beam have a small spread in their natural (synchrotron or betatron) frequencies. The purpose of the present chapter is to introduce this important topic. Section 5.1 describes the physical origin of Landau damping. The results are applied in Section 5.2 to demonstrate Landau damping of bunched beams in circular accelerators, using a macroparticle model. Sections 5.3 and 5.4 then describe the Landau damping of unbunched beams. Finally, in Section 5.5 we briefly discuss a quantity called the beam transfer function.

The theory of Landau damping of unbunched beams was first formulated using the Vlasov technique by Neil and Sessler[2] for the longitudinal case and by Lasslet, Neil, and Sessler[3] for the transverse case. In this chapter, we will proceed with a somewhat different treatment, postponing the Vlasov treatment until Chapter 6. For bunched beams, we consider only a macroparticle model. Landau damping of bunched beams in general (not just for macroparticle models) using the Vlasov technique is beyond the scope of this book.[4]

[1] L. D. Landau, J. Phys. USSR **10**, 25 (1946).
[2] V. Kelvin Neil and Andrew M. Sessler, Rev. Sci. Instr. **6**, 429 (1965).
[3] L. Jackson Laslett, V. Kelvin Neil, and Andrew M. Sessler, Rev. Sci. Instr. **6**, 46 (1965).
[4] G. Besnier, Nucl. Instr. Meth. **164**, 235 (1979); B. Zotter, CERN Report SPS/81-19 (DI) (1981); Yongho Chin, Kohtaro Satoh, and Kaoru Yokoya, Part. Accel. **13**, 45 (1983).

In an accelerator, the spread in natural frequency of the beam comes from several sources. A dependence of the betatron frequency ω_β on the energy of the particle, together with an energy spread in the beam, leads to a spread in ω_β. Nonlinearities in the focusing system cause a dependence of ω_β on the particle's betatron amplitude. A spread in betatron amplitudes then leads also to a spread in ω_β.[5] In the longitudinal case the source of frequency spread depends on whether the beam is bunched or unbunched. For bunched beams, a spread in the synchrotron frequency ω_s can result from nonlinearity in the rf focusing voltage. For unbunched beams, dependence of the revolution frequency on the particle energy plays a similar role. In the following, for all cases studied, we will simply assume a frequency spread specified by an externally given beam frequency spectrum.

5.1 PHYSICAL ORIGIN

Consider a simple harmonic oscillator which has a natural frequency ω. Let this oscillator be driven, starting at time $t = 0$, by a sinusoidal force of frequency Ω. The equation of motion is

$$\ddot{x} + \omega^2 x = A \cos \Omega t \tag{5.2}$$

with the initial conditions $x(0) = 0$ and $\dot{x}(0) = 0$. The solution is

$$x(t > 0) = -\frac{A}{\Omega^2 - \omega^2}(\cos \Omega t - \cos \omega t). \tag{5.3}$$

In Eq. (5.3), the $\cos \Omega t$ term gives the main term responding to the driving force; the $\cos \omega t$ term comes from matching the initial conditions.

Following a treatment by Hereward,[6] Eq. (5.3) is our starting point for the Landau damping analysis. In particular, we will see that the explicit inclusion of the initial conditions plays an important role. Otherwise, one could have

[5]In the following, we assume the spread in ω_β is independent of the amplitude of excitation due to the instability. This will not be true if the ω_β spread is caused by nonlinearities. This subtlety, however, will not be pursued. Interested reader may refer to H. G. Hereward, CERN Report MPS/DL 69-11 (1969), where it is shown that the equivalent of Eq. (5.7) reads

$$\langle x \rangle = -\frac{\pi}{2} A e^{-i\Omega t} \int_0^\infty dJ \frac{J\rho'(J)}{\omega(J) - \Omega}, \tag{5.1}$$

where $J = x^2 + (\dot{x}/\omega)^2$ is the betatron action, and $\rho(J)$ is the unperturbed phase space density normalized by $\int_0^\infty \pi\, dJ[\omega(J) + J\omega'(J)]\rho(J) = 1$. Nonlinearity is characterized by $\omega'(J) \neq 0$.

[6]H. G. Hereward, CERN Report 65-20 (1965). See also A. Hoffmann, CERN Accel. School, Advanced Accel. Phys., CERN Report 89-01 (1989), p. 40; A. Hofmann, *Frontiers of Part. Beams: Intensity Limitations*, Hilton Head Island, Lectures in Phys. **400**, Springer-Verlag, 1990, p. 110.

hastily written down the solution

$$x(t) = -\frac{A}{\Omega^2 - \omega^2}\cos \Omega t \quad \text{or} \quad x(t) = -\frac{A}{\Omega^2 - \omega^2}e^{-i\Omega t}. \tag{5.4}$$

The main difference between Eqs. (5.4) and (5.3) is that Eq. (5.4) contains a singularity at $\Omega = \omega$ while Eq. (5.3) is well behaved there. This singularity is the source of many subtleties and at this point is to be avoided. As we will see later, by applying some mathematical tricks, it is possible to bypass the explicit inclusion of the initial conditions and go straight to Eq. (5.4), but at this point, it is more appropriate to use the well-behaved expression (5.3).

Consider now an ensemble of oscillators (each oscillator represents a single particle in the beam) which do not interact with each other and have a spectrum of natural frequency ω with a distribution $\rho(\omega)$ satisfying $\int_{-\infty}^{\infty} d\omega\, \rho(\omega) = 1$. Now starting at time $t = 0$, subject this ensemble of particles to the driving force $A \cos \Omega t$ with all particles starting with initial conditions $x(0) = 0$ and $\dot{x}(0) = 0$. We are interested in the ensemble average of the response, which is given by superposition,

$$\langle x \rangle (t > 0) = -\int_{-\infty}^{\infty} d\omega\, \rho(\omega) \frac{A}{\Omega^2 - \omega^2}(\cos \Omega t - \cos \omega t). \tag{5.5}$$

In a single-particle response (5.3), the main $\cos \Omega t$ term is in phase (i.e., no $\sin \Omega t$ term) and in frequency relative to the driving force, but the initial condition $\cos \omega t$ term is out of frequency. It seems as if the main ensemble response to the driving force were

$$-\cos \Omega t \int_{-\infty}^{\infty} d\omega\, \rho(\omega) \frac{A}{\Omega^2 - \omega^2}, \tag{5.6}$$

which is in phase and in frequency with the driving force. Equation (5.6) is in fact what we would obtain if we used Eq. (5.4) instead of Eq. (5.3) for the response of single particles. But this observation is incorrect. When the beam spectrum covers the driving frequency Ω, there is a singularity at $\Omega = \omega$. This singularity, when treated properly, contributes to a $\sin \Omega t$ term that is out of phase with the driving force. What is more, this mysterious $\sin \Omega t$ component has a definite sign, which in turn has important consequences.

To observe the $\sin \Omega t$ component, it is necessary to use the complete expression (5.3). For simplicity, let us consider a narrow beam spectrum around a frequency ω_x and a driving frequency near the spectrum, i.e., $\Omega \approx \omega_x$.[7] The beam response is then

$$\langle x \rangle (t) = -\frac{A}{2\omega_x} \int d\omega\, \rho(\omega) \frac{1}{\Omega - \omega}(\cos \Omega t - \cos \omega t). \tag{5.7}$$

[7]Depending on whether the betatron or synchrotron dimension is of interest, ω_x will be taken to be ω_β or ω_s. The coordinate x will be chosen similarly.

Changing variable from ω to $u = \omega - \Omega$ leads to

$$\begin{aligned}\langle x\rangle(t) &= \frac{A}{2\omega_x}\int_{-\infty}^{\infty} du\,\frac{\rho(u+\Omega)}{u}\left[\cos\Omega t - \cos(\Omega t + ut)\right] \\ &= \frac{A}{2\omega_x}\left[\cos\Omega t\int_{-\infty}^{\infty} du\,\rho(u+\Omega)\frac{1-\cos ut}{u}\right. \\ &\qquad \left. +\sin\Omega t\int_{-\infty}^{\infty} du\,\rho(u+\Omega)\frac{\sin ut}{u}\right]. \end{aligned} \tag{5.8}$$

In the above manipulations, we have made sure that all integrals are well behaved at $u = 0$.

Equation (5.8) contains a $\cos\Omega t$ term and a $\sin\Omega t$ term, but their coefficients are time dependent. The next step is to show that those coefficients approach well-behaved limits, and particularly that the $\sin\Omega t$ coefficient does not approach zero. To do so, one first observes

$$\begin{aligned}\lim_{t\to\infty}\frac{\sin ut}{u} &= \pi\delta(u), \\ \lim_{t\to\infty}\frac{1-\cos ut}{u} &= \text{P.V.}\left(\frac{1}{u}\right).\end{aligned} \tag{5.9}$$

The proof of Eq. (5.9) is illustrated in Figure 5.1. As t increases, one notes that $(\sin ut)/u$ peaks around $u = 0$ with increasing height and decreasing width. The area under the function is a constant, given by π, for all t. A moment's reflection verifies the first member of Eq. (5.9). Similarly, as t increases, the function $(1 - \cos ut)/u$ approaches $1/u$ to increasing accuracy around $u = 0$, as shown in Figure 5.1(b). The sole function of the $\cos ut$ term, which oscillates rapidly as $t \to \infty$, is to avoid the singularity at $u = 0$. Recalling the definition of principal values (see Footnote 26 of Chapter 2) proves the second member of Eq. (5.9). Note that Eq. (5.9) is applied only when an integral over u is to be taken next.

If we are not interested in the transient effects immediately following the onset of the driving force, we may substitute Eq. (5.9) into Eq. (5.8) and obtain

$$\langle x\rangle(t) = \frac{A}{2\omega_x}\left[\cos\Omega t\ \text{P.V.}\int d\omega\,\frac{\rho(\omega)}{\omega-\Omega} + \pi\rho(\Omega)\sin\Omega t\right]. \tag{5.10}$$

This expression now contains explicitly a $\cos\Omega t$ term and, as promised, also a $\sin\Omega t$ term.

The sign of the $\cos\Omega t$ term relative to the driving force depends on the sign of $\text{P.V.}\int d\omega\,\rho(\omega)/(\omega - \Omega)$. Generally, this term is approximately given

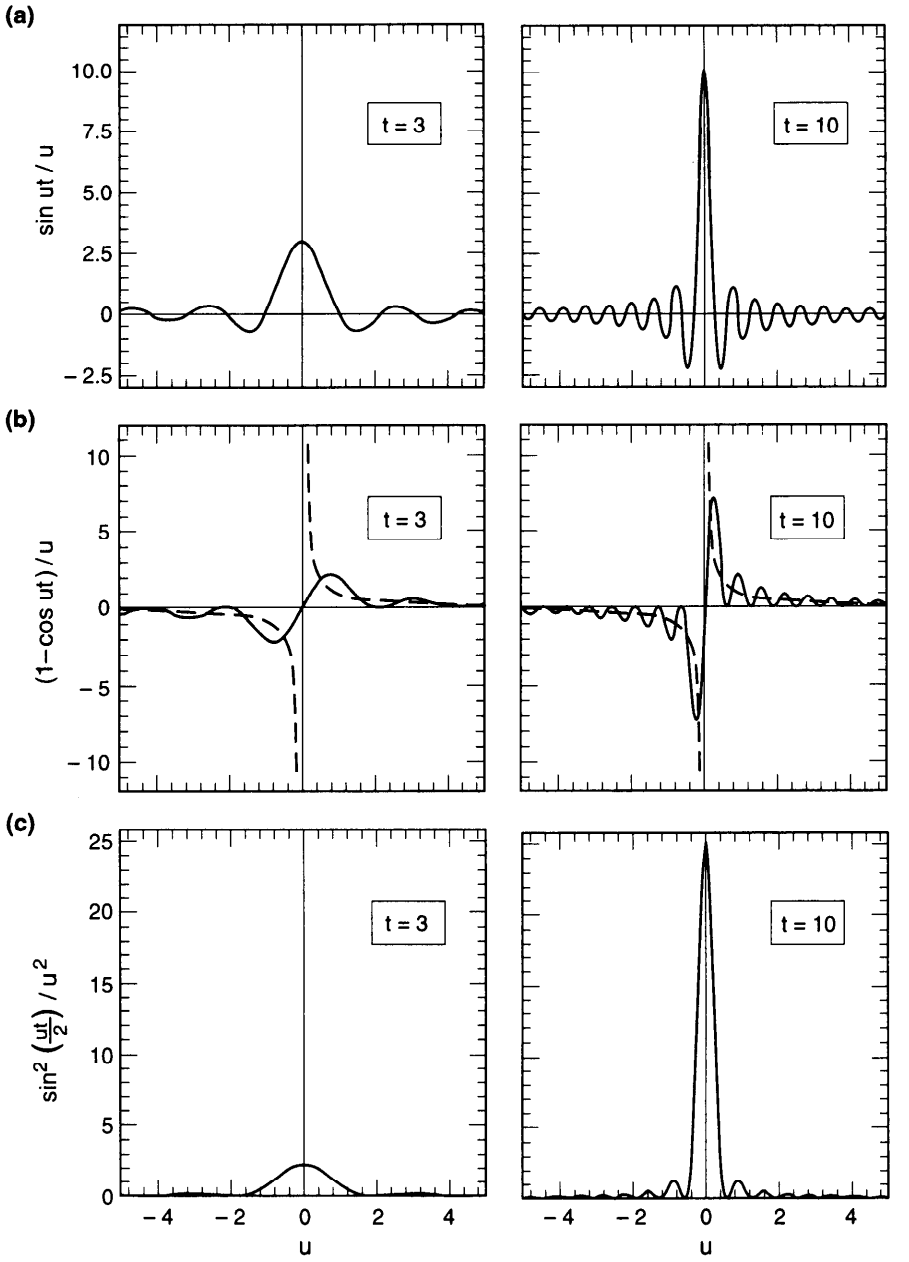

Figure 5.1. The functions $\sin(ut)/u$, $(1-\cos ut)/u$, and $\sin^2(ut/2)/u^2$ are shown in (a), (b), and (c) for two values $t = 3$ and 10. The dashed curves in (b) are for the function $1/u$.

by $1/(\omega_x - \Omega)$ outside the spectrum and crosses through zero somewhere inside the spectrum. (See Figure 5.3 below for examples). A system is referred to as "capacitive" or "inductive" based on whether its sign is positive or negative.

The $\sin \Omega t$ term has a definite sign relative to the driving force, because $\rho(\Omega)$ is always positive. In particular, $d\langle x\rangle/dt$ is always in phase with the force, indicating work is being done on the system. The system always reacts to the force "resistively."

Exercise 5.1 In case the driving force is $A\cos(\Omega t + \phi)$, follow the steps leading to Eq. (5.10) to show that the asymptotic beam response is

$$\langle x\rangle(t) = \frac{A}{2\omega_x}\left[\cos(\Omega t + \phi)\text{P.V.}\int d\omega\,\frac{\rho(\omega)}{\omega - \Omega} + \pi\rho(\Omega)\sin(\Omega t + \phi)\right]. \tag{5.11}$$

Other than replacing Ωt by $\Omega t + \phi$, the only difference in beam response from the case when $\phi = 0$ is in the transients.

The Landau damping effect is to be distinguished from a *decoherence* (also called phase-mixing, or filamentation) effect that occurs when the beam has nonzero initial conditions. Had we included an initial condition $x(0) = x_0$ and $\dot{x}(0) = \dot{x}_0$, we would have introduced two additional terms into the ensemble response:

$$x_0\int d\omega\,\rho(\omega)\cos\omega t + \dot{x}_0\int d\omega\,\rho(\omega)\frac{\sin\omega t}{\omega}. \tag{5.12}$$

These terms do not participate in the dynamic interaction of the beam particles and are not very interesting for our purposes here. In this decoherence effect, individual particles continue to execute oscillations of constant amplitude, but the total beam response $\langle x\rangle$ decreases with time.[8]

As mentioned, work is continuously being done on the system. However, the amplitude of $\langle x\rangle$, as given in Eq. (5.10), does not increase with time. Where did the energy go? To investigate this, let us first identify the energy of a particle as the square of its oscillation amplitude. From Eq. (5.3), the amplitude of a particle is given by the slowly varying envelope

$$\text{amplitude} = \frac{A}{\omega_x(\Omega - \omega)}\sin\frac{(\Omega - \omega)t}{2}. \tag{5.13}$$

[8]Provided $\rho(\omega) = 0$ at $\omega = 0$. See Exercise 5.2(b).

This leads to a total oscillation energy of

$$\mathscr{E} = N\int d\omega\, \rho(\omega)\left[\frac{A}{\omega_x(\Omega-\omega)}\sin\frac{(\Omega-\omega)t}{2}\right]^2$$

$$= \frac{NA^2}{\omega_x^2}\int du\, \rho(u+\Omega)\frac{\sin^2(ut/2)}{u^2}, \tag{5.14}$$

where N is the total number of particles in the beam. Figure 5.1(c) shows the behavior of $\sin^2(ut/2)/u^2$. As t increases, the region where this function assumes significant values narrows around $u = 0$. The range of the region decreases as $1/t$, but the height of the function increases quadratically as t^2, leading to an area under the function that increases linearly with t. In fact,

$$\lim_{t\to\infty}\frac{\sin^2(ut/2)}{u^2} = \frac{\pi t}{2}\delta(u). \tag{5.15}$$

Equation (5.14) then reads

$$\mathscr{E} = \frac{\pi}{2}\frac{NA^2}{\omega_x^2}\rho(\Omega)t, \tag{5.16}$$

which increases linearly with time. The system therefore absorbs energy from the driving force indefinitely while holding the ensemble beam response within bounds.

An analogy occurs in the decoherence behavior described by Eq. (5.12). In that case, the single-particle energies and thus the total beam energy are constant in time, but the ensemble signal $\langle x\rangle$ decreases with time.

The stored energy (5.16) is incoherent in the sense that the energy is contained in the individual particles, but it is not to be regarded as heat in the system. This is because the stored energy is not distributed more or less uniformly in all particles, but is selectively stored in particles with continuously narrowing range of frequencies around the driving frequency. Figure 5.2 shows the driving force and the single-particle responses (5.3) for different particle frequencies. One sees that a particle with $\omega = \Omega$, being resonantly driven, continues to increase in amplitude as t increases. A particle with ω away from Ω gets out of resonance after a time approximately $\pi/|\omega - \Omega|$, and at time $t = 2\pi/|\omega - \Omega|$, the particle returns all its energy back to the driving force in a beating process.

It is mainly those particles with $|\omega - \Omega| < 1/t$ that contribute to the $\sin\Omega t$ response, and those particles with $|\omega - \Omega| > 1/t$ that contribute to the $\cos\Omega t$ response. Since the number of particles with $|\omega - \Omega| < 1/t$ decreases with time as $1/t$ while their amplitude increases as t, the net $\sin\Omega t$ contribution to $\langle x\rangle$ is constant in time.

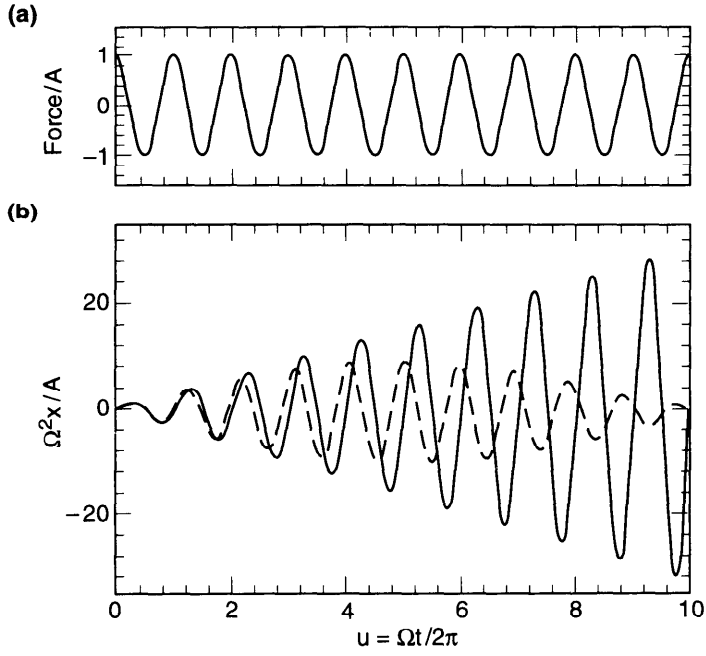

Figure 5.2. Single-particle response $x(t)$ to a sinusoidal driving force $f(t) = A\cos\Omega t$. (a) $f(t)/A$ versus $\upsilon = \Omega t/2\pi$; (b) $\Omega^2 x(t)/A$ versus υ. The solid curve is for a particle on resonance with $\omega = \Omega$. The dashed curve is for a particle with $\omega = 1.1\Omega$.

The asymptotic behavior (5.10) applies if one waits for a time longer than $1/\Delta\omega$, where $\Delta\omega$ is the frequency spread of the beam spectrum. For $t < 1/\Delta\omega$, the beam response is confounded by transient terms. Furthermore, the $\sin\Omega t$ term is proportional to $\rho(\Omega)$. If the spectrum is such that there are no particles near frequency Ω to continuously absorb energy, Landau damping will cease and a beating phenomenon takes over. Since a beam consists of a finite number of particles, Landau damping will cease when t is larger than $1/\delta\omega$, where $\delta\omega$ is the frequency spacing between two nearest particles. The range of time for Eq. (5.10) to be applicable is therefore

$$\frac{1}{\delta\omega} \gg t \gg \frac{1}{\Delta\omega}. \tag{5.17}$$

With N particles in the beam, one might have $\delta\omega \approx \Delta\omega/N$. Taking $N = 10^{11}$ and $\Delta\omega = 10^3\ \mathrm{s}^{-1}$ for example, the time is limited to the range between 1 ms and 10^8 s.

Of course the upper limit can be exceeded long before 10^8 s if the resonant particles are lost when their amplitudes exceed b, the radius of the vacuum chamber. Using Eq. (5.13), this occurs when $At/2\omega_x > b$. The

applicable time for Landau damping then becomes

$$\frac{2b\omega_x}{A} > t \gg \frac{1}{\Delta\omega}. \tag{5.18}$$

An alternative way to consider the beam response that avoids the consideration of transient effects (and therefore removes the limit $t \gg 1/\Delta\omega$) is to pretend that the driving force has been in existence since $t \to -\infty$, except that the force contains an extra exponential factor $e^{\epsilon t}$ which goes to 0 as $t \to -\infty$, i.e., the force has been turned on adiabatically. This extra exponential factor effectively takes into account the initial conditions while removing the transient effects. The price to pay is that the force then grows indefinitely as $t \to \infty$. Fortunately it is just the slightly growing solutions that most interest us, because they correspond to the situation when the beam is at the edge of instability. These considerations will be elaborated upon as the subject of Landau damping is developed.

In the following, we give several explicit examples, the first of which is when all particles in the beam have the same natural frequency, i.e.,

$$\rho(\omega) = \delta(\omega - \omega_x). \tag{5.19}$$

In this trivial case, we have the following asymptotic beam response to a driving force $A \cos \Omega t$:

$$\langle x \rangle = \frac{A}{2\omega_x}\left[\frac{\cos \Omega t}{\omega_x - \Omega} + \pi\delta(\Omega - \omega_x)\sin \Omega t\right]. \tag{5.20}$$

The first nontrivial case to be considered is for a Lorentz spectrum

$$\rho(\omega) = \frac{\Delta\omega}{\pi}\frac{1}{(\omega - \omega_x)^2 + \Delta\omega^2}. \tag{5.21}$$

We have[9]

$$\text{P.V.}\int d\omega \frac{\rho(\omega)}{\omega - \Omega} = \frac{\omega_x - \Omega}{(\omega_x - \Omega)^2 + \Delta\omega^2}. \tag{5.22}$$

Substituting into Eq. (5.10) yields the beam response

$$\langle x \rangle = \frac{A}{2\omega_x}\frac{(\omega_x - \Omega)\cos \Omega t + \Delta\omega \sin \Omega t}{(\omega_x - \Omega)^2 + \Delta\omega^2}. \tag{5.23}$$

[9]Derivation of Eq. (5.22) is omitted here. It can be obtained by a complex variable technique or by applying Eq. (2.95).

The system is purely resistive if driven on resonance with $\Omega = \omega_x$, capacitive if $\Omega < \omega_x$, and inductive if $\Omega > \omega_x$.

Exercise 5.2

(a) Equation (5.23) gives the asymptotic behavior when $t \gg 1/\Delta\omega$. Show that, for the Lorentz spectrum, the exact expression including the transient effect is

$$\begin{aligned}\langle x\rangle(t) = {} & \frac{A}{2\omega_x\left[(\omega_x - \Omega)^2 + \Delta\omega^2\right]} \\ & \times\Big\{\cos\Omega t\left[\omega_x - \Omega - \Delta\omega\, e^{-\Delta\omega t}\sin(\omega_x t - \Omega t)\right. \\ & \qquad \left. + (\omega_x - \Omega)e^{-\Delta\omega t}\cos(\omega_x t - \Omega t)\right] \\ & + \sin\Omega t\left[\Delta\omega - \Delta\omega\, e^{-\Delta\omega t}\cos(\omega_x t - \Omega t)\right. \\ & \qquad \left. - (\omega_x - \Omega)e^{-\Delta\omega t}\sin(\omega_x t - \Omega t)\right]\Big\}, \quad (5.24)\end{aligned}$$

which reduces to Eq. (5.23) when $t \gg 1/\Delta\omega$. The fact that the transient terms decay exponentially is specific to the Lorentz spectrum. A different spectrum would give a different time dependence of the transients, but the general conclusion is still valid that they decay when $t \gg 1/\Delta\omega$ for a distribution with frequency spread $\Delta\omega$.

(b) Show that the decoherence term (5.12) for a Lorentz spectrum is

$$\begin{aligned}\langle x\rangle(t) = {} & e^{-\Delta\omega t}\left(x_0\cos\omega_x t - \dot{x}_0\frac{\Delta\omega\cos\omega_x t - \omega_x\sin\omega_x t}{\omega_x^2 + \Delta\omega^2}\right) \\ & + \frac{\Delta\omega\,\dot{x}_0}{\omega_x^2 + \Delta\omega^2}. \quad (5.25)\end{aligned}$$

Note that $\langle x\rangle$ does not approach zero as $t \to \infty$. This comes from particles with $\omega \to 0$; with $\dot{x}_0 \neq 0$, their amplitudes increase indefinitely. The decoherence signal decays only when $\rho(0) = 0$.

For a general beam frequency spectrum, we parametrize the asymptotic beam response as

$$\langle x\rangle = \frac{A}{2\omega_x\,\Delta\omega}\left[f(u)\cos\Omega t + g(u)\sin\Omega t\right], \quad (5.26)$$

where we have introduced

$$f(u) = \Delta\omega \,\text{P.V.} \int d\omega \, \frac{\rho(\omega)}{\omega - \Omega},$$
$$g(u) = \pi \Delta\omega \, \rho(\omega_x - u \, \Delta\omega), \tag{5.27}$$
$$u = \frac{\omega_x - \Omega}{\Delta\omega}.$$

In this notation, we have for the δ-function spectrum

$$f(u) = \frac{1}{u} \quad \text{and} \quad g(u) = \pi\delta(u), \tag{5.28}$$

and for the Lorentz spectrum

$$f(u) = \frac{u}{1 + u^2} \quad \text{and} \quad g(u) = \frac{1}{1 + u^2}. \tag{5.29}$$

A few more examples of different frequency spectra are given below. For a rectangular spectrum

$$\rho(v) = \frac{1}{2\,\Delta\omega} H(1 - |v|), \qquad v = \frac{\omega_x - \omega}{\Delta\omega}, \tag{5.30}$$

where $H(x)$ is the step function $H(x) = 1$ if $x > 0$ and 0 if $x < 0$, the asymptotic beam response is described by

$$f(u) = \frac{1}{2} \ln\left|\frac{u + 1}{u - 1}\right| \quad \text{and} \quad g(u) = \frac{\pi}{2} H(1 - |u|). \tag{5.31}$$

For a parabolic spectrum, we have

$$\rho(v) = \frac{3}{4\,\Delta\omega}(1 - v^2) H(1 - |v|),$$
$$f(u) = \frac{3}{4}\left[(1 - u^2)\ln\left|\frac{u + 1}{u - 1}\right| + 2u\right], \tag{5.32}$$
$$g(u) = \frac{3\pi}{4}(1 - u^2) H(1 - |u|).$$

For an elliptical spectrum, we have

$$\begin{aligned} \rho(v) &= \frac{2}{\pi \Delta\omega} H(1 - |v|)\sqrt{1 - v^2}, \\ f(u) &= 2\left[u - \operatorname{sgn}(u) H(|u| - 1)\sqrt{u^2 - 1}\right], \\ g(u) &= 2H(1 - |u|)\sqrt{1 - u^2}. \end{aligned} \tag{5.33}$$

For a bi-Lorentz spectrum, we have

$$\begin{aligned} \rho(v) &= \frac{2}{\pi \Delta\omega(v^2 + 1)^2}, \\ f(u) &= \frac{u(u^2 + 3)}{(u^2 + 1)^2}, \\ g(u) &= \frac{2}{(u^2 + 1)^2}. \end{aligned} \tag{5.34}$$

And, finally, for a Gaussian spectrum, we have

$$\begin{aligned} \rho(v) &= \frac{1}{\sqrt{2\pi}\,\Delta\omega} e^{-v^2/2}, \\ f(u) &= \sqrt{\frac{2}{\pi}}\, e^{-u^2/2} \int_0^\infty \frac{dy}{y} e^{-y^2/2} \sinh(uy), \\ g(u) &= \sqrt{\frac{\pi}{2}}\, e^{-u^2/2}. \end{aligned} \tag{5.35}$$

The function $f(u)$ for the Gaussian spectrum is approximately equal to u for small u and to $1/u$ for large u.

Figure 5.3 shows the functions f and g for the various spectra. The function g is simply related to the spectrum by $\rho = g/(\pi \Delta\omega)$, and the function f is related to the principle value integral over the spectra. An inspection of Figure 5.3 indicates that $f(u)$ resembles $-g'(u)$. The reason for this behavior should become clear on inspecting the principle value integral expression for $f(u)$.

Exercise 5.3 Although $f(u)$ resembles $-g'(u)$, show that no realistic spectrum gives $f(u) \propto -g'(u)$ exactly.

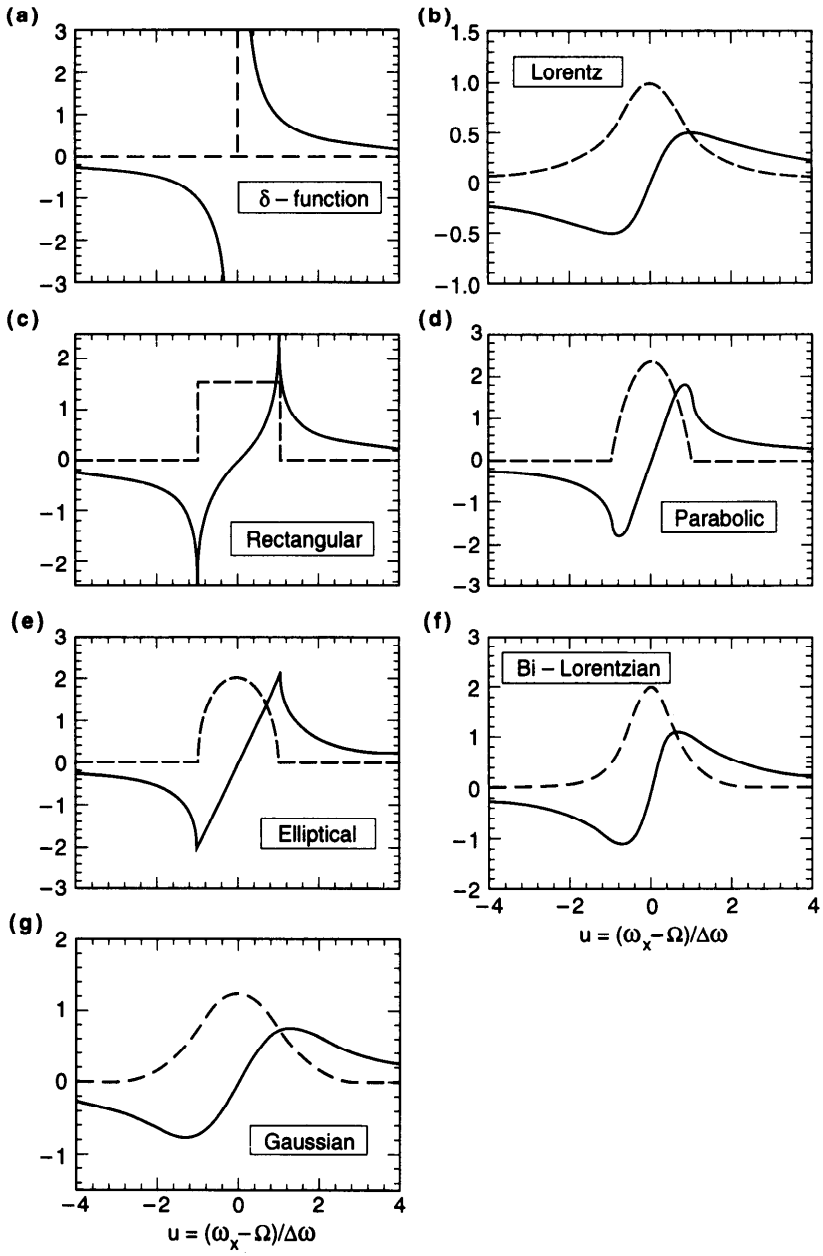

Figure 5.3. The functions $f(\upsilon)$ (solid curves) and $g(\upsilon)$ (dashed curves) versus $\upsilon = (\omega_x - \Omega)/\Delta\omega$ for various beam frequency spectra. The shape of the spectra is the same as the dashed curves.

Exercise 5.4 Show for the above examples that when $|\Omega - \omega_x| \gg \Delta\omega$, the entire beam responds to the driving force as a single particle, with $\langle x \rangle$ given by Eq. (5.4).

To proceed, let us write the beam response (5.10) in a complex notation, which we have tried to avoid so far, keeping in mind that only the real parts are meaningful:

$$\text{driving force} = Ae^{-i\Omega t},$$

$$\langle x \rangle = \frac{A}{2\omega_x} e^{-i\Omega t}\left[\text{P.V.}\int d\omega \, \frac{\rho(\omega)}{\omega - \Omega} + i\pi\rho(\Omega)\right] \tag{5.36}$$

$$= \frac{A}{2\omega_x \, \Delta\omega} e^{-i\Omega t}[f(u) + ig(u)],$$

where $u = (\omega_x - \Omega)/\Delta\omega$. In this expression, one could include a phase in the driving force by considering a complex A. (See Exercise 5.1.) We will refer to the dimensionless complex quantity $f + ig$ as the *beam transfer function* (BTF), which is the subject of Section 5.5 below.

Having demonstrated the detailed treatment of the initial conditions, the apparent singularities, and the out-of-phase beam responses, we are now ready to introduce a mathematical trick which bypasses most of these subtleties and makes the analysis much more concise. It turns out that one can "derive" the same result by venturing with the response (5.4). In complex notation, the single-particle motion (5.4) gives a total beam response

$$\langle x \rangle = \frac{A}{2\omega_x} e^{-i\Omega t} \int d\omega \, \frac{\rho(\omega)}{\omega - \Omega}. \tag{5.37}$$

The detailed examinations so far now provide a well-defined way to deal with the otherwise undefined integral in Eq. (5.37), namely, we are supposed to make the connection

$$\int d\omega \, \frac{\rho(\omega)}{\omega - \Omega} \to \text{P.V.}\int d\omega \, \frac{\rho(\omega)}{\omega - \Omega} + i\pi\rho(\Omega), \tag{5.38}$$

or more symbolically

$$\frac{1}{\omega - \Omega} \to \text{P.V.}\left(\frac{1}{\omega - \Omega}\right) + i\pi\delta(\omega - \Omega). \tag{5.39}$$

Again, it is necessary to include an out-of-phase term—with a definite sign—as evidenced by the imaginary term $i\pi\rho(\Omega)$ in Eq. (5.38), even though the expression on the left hand side seems to be for a real quantity.

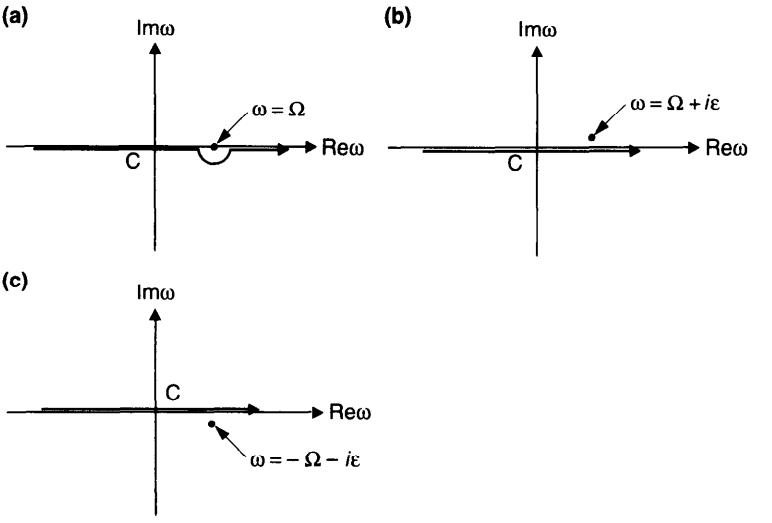

Figure 5.4. Contours in the complex ω-plane: (a) for Eq. (5.40); (b) for Eq. (5.41); (c) for Eq. (5.45) when $\Omega < 0$. The contours can be closed either in the upper half plane or the lower half plane provided $\rho(\omega)$ converges sufficiently rapidly as $|\omega| \to \infty$.

The right hand side of Eq. (5.38) in fact is equal to the left hand side provided one takes the integration to be executed in the complex ω-plane and the contour of integration, C, is as illustrated in Figure 5.4(a). The connection (5.38) now reads

$$\int d\omega \frac{\rho(\omega)}{\omega - \Omega} \to \int_C d\omega \frac{\rho(\omega)}{\omega - \Omega}. \tag{5.40}$$

The straight line portion of C gives the principal value term in $\langle x \rangle$, and the semicircular portion gives the pole contribution $i\pi\rho(\Omega)$.

Equivalently one could consider the integration along the real axis of the ω-plane, but move the pole at $\omega = \Omega$ up by an infinitesimal amount. This leads to an alternative expression

$$\int d\omega \frac{\rho(\omega)}{\omega - \Omega} \to \int_{-\infty}^{\infty} d\omega \frac{\rho(\omega)}{\omega - \Omega - i\epsilon}, \tag{5.41}$$

or

$$\frac{1}{\omega - \Omega} \to \frac{1}{\omega - \Omega - i\epsilon}, \tag{5.42}$$

or simply

$$\Omega \to \Omega + i\epsilon. \tag{5.43}$$

The connection (5.43) has the physical meaning of considering a force that has a time dependence of $\exp(-i\Omega t + \epsilon t)$, i.e., a force that grows with time at an infinitesimal rate. This means the driving force has not been in existence since $t = -\infty$, which has the same effect as introducing explicit initial conditions as far as removing the singularity is concerned.

Exercise 5.5 Establish the equivalence between Eq. (5.42) and Eq. (5.39) by explicitly showing that the real part of $(\omega - \Omega - i\epsilon)^{-1}$ gives P.V.$(\omega - \Omega)^{-1}$, and the imaginary part is equal to $\pi\delta(\omega - \Omega)$.

Exercise 5.6 In case one has to consider a driving force $Ae^{-i\Omega t}$ with a negative frequency $\Omega < 0$ and a spectrum that peaks around $\omega_x > 0$, the singularity will be located at $\omega = -\Omega = |\Omega|$. Follow the steps leading to Eq. (5.38) to show that

$$\langle x \rangle = \frac{A}{2\omega_x}\left[\cos \Omega t \ \text{P.V.}\int \frac{\rho(\omega)}{\omega + \Omega} - \pi\rho(|\Omega|)\sin \Omega t\right], \tag{5.44}$$

or

$$\int d\omega \frac{\rho(\omega)}{\omega + \Omega} \to \text{P.V.}\int d\omega \frac{\rho(\omega)}{\omega - |\Omega|} - i\pi\rho(|\Omega|). \tag{5.45}$$

The imaginary part has switched sign from Eq. (5.38). The contour C will now make an excursion above the pole at $\omega = -\Omega$ as shown in Figure 5.4(c), which means the connection (5.43) is maintained. Show that the $\sin \Omega t$ component gives rise to a $d\langle x \rangle/dt$ term which is in phase with the driving force, indicating the system is absorbing energy from the driving force.

It is now a matter of taste whether to regard our main conclusion (5.38) as a result of a simple derivation starting with Eq. (5.4) and then make an educated connection (5.40) or (5.43), or to regard it as a result of a detailed calculation which takes account of initial conditions.

We proceed in the remainder of this chapter to demonstrate Landau damping of collective instabilities in circular accelerators.

5.2 ONE-PARTICLE MODEL FOR BUNCHED BEAMS

Results obtained in the previous section, when applied to circular accelerators, lead to Landau damping of collective instabilities. To demonstrate this for a bunched beam, consider a one-particle model in which the bunched beam is a single macroparticle of charge Ne, as we did in Section 4.2, except

now the N individual particles have a spread in their natural frequencies. The fact that they form one macroparticle even though they have different frequencies is a result of the bunch executing a collective motion.

The driving force on the individual particles comes from the center-of-charge displacement of the beam as a whole, $\langle y \rangle$. Equation (4.24) is therefore slightly modified to give, for a single particle whose betatron frequency is ω,

$$y''(s) + \left(\frac{\omega}{c}\right)^2 y(s) = -\frac{Nr_0}{\gamma C} \sum_{k=1}^{\infty} \langle y \rangle (s - kC) W_1(-kC). \quad (5.46)$$

Consider the situation when the vertical betatron y-motion of the macroparticle is just at the edge of exponential growth due to a collective instability. We have

$$\langle y \rangle (s) = Be^{-i\Omega s/c}. \quad (5.47)$$

Because we are considering the case when the beam is at the edge of instability, we let Ω to carry an imaginary part $i\epsilon$, where ϵ is infinitesimally positive, as prescribed by Eq. (5.43).

It is not very interesting to search for damped, stable solutions. Instability occurs when there are antidamped solutions, irrespective of how many damped solutions there may be. Finding stable solutions does not assure beam stability, but finding one unstable solution reveals the beam to be unstable.

Substituting Eq. (5.47) into Eq. (5.46) gives

$$y''(s) + \left(\frac{\omega}{c}\right)^2 y(s) = -\frac{BNr_0}{\gamma C} \mathscr{W} e^{-i\Omega s/c}, \quad (5.48)$$

where we have defined a complex quantity

$$\mathscr{W} = \sum_{k=1}^{\infty} W_1(-kC) e^{i\omega_\beta k T_0}, \quad (5.49)$$

or in terms of impedance,

$$\mathscr{W} = -\frac{i}{T_0} \sum_{p=-\infty}^{\infty} Z_1^{\perp}(p\omega_0 + \omega_\beta). \quad (5.50)$$

In writing down Eqs. (5.49–5.50), we have used the notation $C/c = T_0 = 2\pi/\omega_0$. We have also assumed the mode frequency shift is small, so that $\Omega \approx \omega_\beta$, where ω_β is the center of the beam frequency spectrum. To assure

the validity of a one-particle model, the mode frequency shift must be much less than the synchrotron frequency ω_s.

Equation (5.48) says that the beam is driven by a force of the form $Ae^{-i\Omega s/c}$ as prescribed in the previous section. Equation (5.36) gives the response of the beam to the driving force, and it reads

$$\langle y \rangle = -\frac{BNr_0 \mathscr{W} c}{2\omega_\beta \gamma T_0} e^{-i\Omega s/c} \left[\text{P.V.} \int d\omega \, \frac{\rho(\omega)}{\omega - \Omega} + i\pi\rho(\Omega) \right]. \quad (5.51)$$

But we have already assumed that the collective beam motion is given by Eq. (5.47). This means the mode frequency Ω is not arbitrary. In order for the beam motion to be nontrivial,[10] Ω must satisfy a self-consistency condition, known as the *dispersion relation*,

$$1 = -\frac{Nr_0 \mathscr{W} c}{2\omega_\beta \gamma T_0} \left[\text{P.V.} \int d\omega \, \frac{\rho(\omega)}{\omega - \Omega} + i\pi\rho(\Omega) \right] \quad (5.52)$$

or, in terms of the function $f(u)$ and $g(u)$ defined in Eq. (5.27),

$$-\frac{Nr_0 \mathscr{W} c}{2\omega_\beta \gamma T_0 \, \Delta\omega} = \frac{1}{f(u) + ig(u)}. \quad (5.53)$$

Exercise 5.7 Find the dispersion relation for a system in which the driving force on individual particles comes from $\langle y \rangle$ according to

$$\ddot{y} + \omega^2 y = W_1 \langle y \rangle + \frac{W_2}{\omega_\beta} \frac{d\langle y \rangle}{dt}, \quad (5.54)$$

where ω_β is the center of the beam frequency spectrum. Compare with Eq. (5.53) to establish a connection between W_1, W_2, and the impedance. Note the sign of W_2 defines the stability of the beam in the absence of Landau damping.

Exercise 5.8 A feedback system can be modeled as

$$\ddot{y}(t) + \omega^2 y(t) = g\langle y \rangle (t - \tau), \quad (5.55)$$

where g is the gain of the feedback system. A resistive feedback system is given by $\tau = \pi/2\omega$. A reactive feedback system has $\tau = 0$ or π/ω. (a) Find the equivalent impedance of the feedback system (5.55). (b) Find the dispersion relation.

[10] A trivial solution means $B = 0$, i.e., the beam does not oscillate.

In Section 4.2, we obtained an expression (4.25) for the complex mode frequency shift in the *absence* of Landau damping, which, denoted as ξ_1, is given by

$$\xi_1 \equiv (\Omega - \omega_\beta)_{\text{no Landau damping}} = \frac{Nr_0 c\mathscr{W}}{2\omega_\beta \gamma T_0}. \tag{5.56}$$

Equation (5.56) contains essentially the beam intensity, multiplied by the impedance, divided by the focusing strength and the particle rigidity. Combining Eqs. (5.53) and (5.56) leads to the dispersion relation

$$-\frac{\xi_1}{\Delta\omega} = \frac{1}{f(u) + ig(u)}. \tag{5.57}$$

The left hand side of Eq. (5.57) contains the information about the beam intensity and the impedance. The right hand side contains information about the beam frequency spectrum. Calculation of the left hand side is straightforward. For a given impedance, one only needs to calculate the complex mode frequency shift ξ_1 in the absence of Landau damping as was done in Section 4.2. Without Landau damping, the condition for the beam to be stable is simply Im $\xi_1 < 0$.

Once its left hand side is obtained, Eq. (5.57) can in principle be used to determine the mode frequency Ω in the presence of Landau damping when the beam is at the edge of instability. However, the exact value of Ω is not a very useful piece of information. The more useful question to ask is under what conditions the beam becomes unstable regardless of the exact value of Ω under these conditions, and Eq. (5.57) can be used in a reversed manner to address this question. To do so, one considers the real parameter $u = (\omega_\beta - \Omega)/\Delta\omega$ and observes the lotus traced out in the complex $\mathscr{D}_1$-plane as u is scanned from ∞ to $-\infty$, where $\mathscr{D}_1$ is the right hand side of Eq. (5.57),

$$\mathscr{D}_1 = \frac{1}{f(u) + ig(u)}. \tag{5.58}$$

This lotus defines a *stability boundary diagram*. The left hand side of Eq. (5.57), a complex quantity, is then plotted in the complex $\mathscr{D}_1$-plane as a single point. If this point lies on the lotus, it means the solution of Ω for Eq. (5.57) is real, and this ξ_1 value is such that the beam is just at the edge of instability. If it lies on the inside of the lotus (the side which contains the origin of the $\mathscr{D}_1$-plane), the beam is stable. If it lies on the outside of the lotus, the beam is unstable.

Figure 5.5 depicts the stability boundary diagrams for various beam frequency spectra. The beam is unstable if $-\xi_1/\Delta\omega$ lies in the shaded regions. In case of the δ-function spectrum, which is the case without Landau

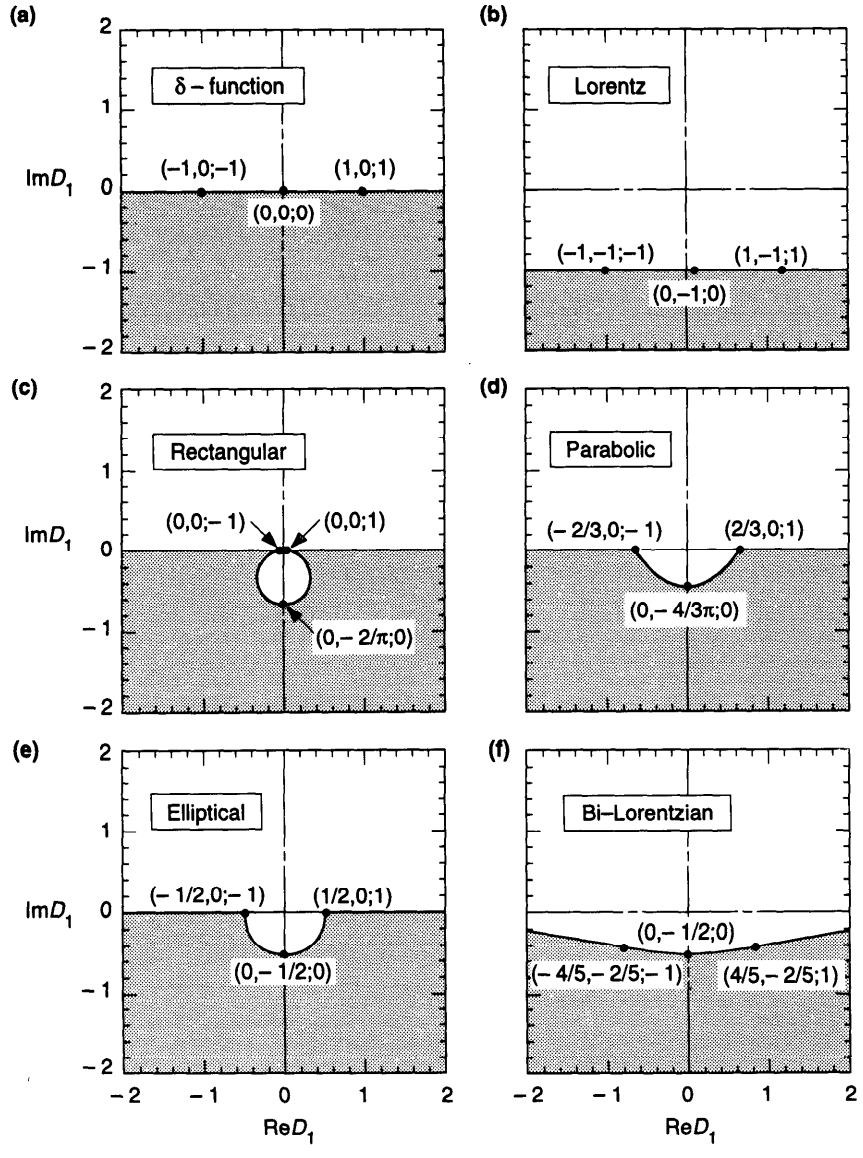

Figure 5.5. The stability boundary diagrams for various spectra in the complex $\mathscr{D}_1$-plane. (a) δ-function spectrum, no Landau damping. (b) Lorentz spectrum. (c) Rectangular spectrum. (d) Parabolic spectrum. (e) Elliptical spectrum. (f) Bi-Lorentzian spectrum. (g) Gaussian spectrum. The boundary for (b) is $\operatorname{Im} \mathscr{D}_1 = -1$. The boundary for (c) contains a displaced circle of radius $1 / \pi$. The boundary for (e) contains a semicircle of radius $\frac{1}{2}$. If the complex quantity $-\xi_1 / \Delta\omega$ lies in a shaded region, the beam is unstable. Three values are assigned to a chosen set of points on the boundaries; they refer to $(\operatorname{Re} \mathscr{D}_1, \operatorname{Im} \mathscr{D}_1; v)$. The value of v can be used to obtain the mode frequency Ω. Case (h) is the simplified criterion (5.62) assuming $\Delta\omega_{1/2} = \sqrt{3}\, \Delta\omega / 2$.

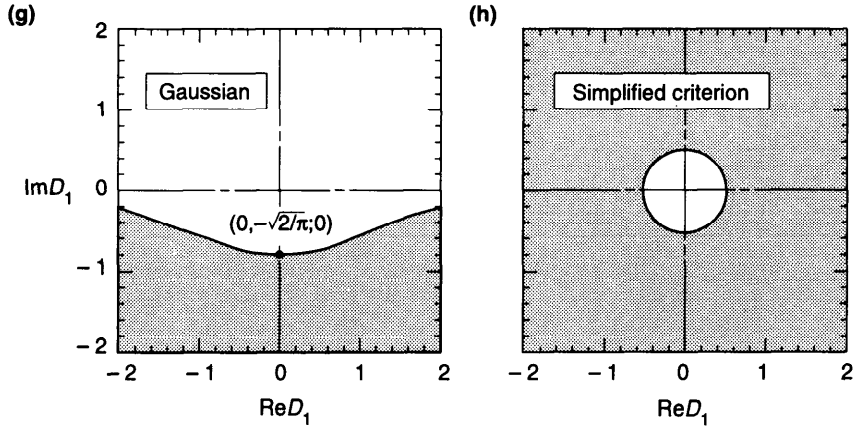

Figure 5.5. *(Continued)*

damping, the stability region reduces to the condition $\text{Im}\,\xi_1 < 0$. All the other cases have larger regions of stability. A finite spread in the natural frequencies thus helps stabilize the beam against collective instabilities, demonstrating the Landau damping mechanism.

Exercise 5.9 It will be instructive to go through the details of how a stability diagram is established.

(a) Either derive one of the examples in the text, or work out a new example such as $\rho(v) \propto (1 - v^2)^2 H(1 - |v|)$, where v and $H(x)$ are defined in Eq. (5.30).

(b) All the spectra so far are symmetric with respect to the spectral center (i.e., even functions of v). Study a case with asymmetric spectrum such as $\rho(v) \propto (1 + v)H(1 - |v|)$ and observe the effect of asymmetry on the stability boundary diagram.

The dispersion relation is particularly simple for the Lorentz spectrum. From Eqs. (5.57) and (5.29), we find

$$\Omega = \omega_\beta + \xi_1 - i\,\Delta\omega. \tag{5.59}$$

The stability condition $\text{Im}\,\Omega < 0$ therefore becomes

$$\text{Im}\,\xi_1 < \Delta\omega, \tag{5.60}$$

which is what appears in the stability diagram, Figure 5.5(b).

The fact that the stable region is always enlarged by the frequency spread can be traced back to the fact that $g(u)$ is always positive. As pointed out in

Section 5.1, this in turn comes from the fact that the beam continues to absorb energy from the driving force without having to let $\langle y \rangle$ grow.

For a given spectral shape, the tolerable ξ_1 is proportional to $\Delta\omega$. The larger the frequency spread, the stronger the Landau damping. Also, for a given $\Delta\omega$, the effectiveness of Landau damping is different for different spectral shapes. Among the spectra shown in Figure 5.5, the Lorentz spectrum, having a long distribution tail, is the most effective; spectra with cutoff tails tend to be less effective, while the δ-function spectrum, of course, is not effective at all. Sharp edges in a spectral shape are reflected in sharp edges in the stability boundary.

To facilitate a more quantitative comparison among different spectra, it may be useful to relate $\Delta\omega$ to the half width at half maximum, $\Delta\omega_{1/2}$, of the various spectra. This is given by

$$\Delta\omega_{1/2} = \Delta\omega \times \begin{cases} 1, & \text{Lorentz,} \\ 1, & \text{rectangular,} \\ \dfrac{1}{\sqrt{2}}, & \text{parabolic,} \\ \dfrac{\sqrt{3}}{2}, & \text{elliptical,} \\ \sqrt{\sqrt{2}-1}, & \text{bi-Lorentzian,} \\ \sqrt{2\ln 2}, & \text{Gaussian.} \end{cases} \tag{5.61}$$

A fair comparison of two spectral shapes is made when they have the same $\Delta\omega_{1/2}$, not the same $\Delta\omega$.

For practical accelerator operations, there may be approximate information on the value of $\Delta\omega_{1/2}$, but not enough detailed information on the shape of the frequency spectrum; or there may be only a need of a rough estimate of whether the collective instability is Landau damped. For those purposes, we introduce a simplified stability criterion as[11]

$$|\xi_1| = \frac{Nr_0 c}{2\omega_\beta \gamma T_0^2} \left| \sum_{p=-\infty}^{\infty} Z_1^{\perp}(p\omega_0 + \omega_\beta) \right| < \frac{1}{\sqrt{3}} \Delta\omega_{1/2}, \tag{5.62}$$

where the factor $1/\sqrt{3}$ is chosen so that it coincides with the semicircular portion of the boundary for the elliptical spectrum. Figure 5.5(h) shows the stability region corresponding to Eq. (5.62). It is to be compared with the stability boundaries for the more realistic spectra shown in Figure 5.5(b) to (g).

[11] This is done in the same spirit as Eq. (5.130) to be discussed later.

Although the exact stability condition depends on details of the spectrum, Eq. (5.62) is an important qualitative result. It says that if the mode frequency shift or growth rate, calculated without Landau damping, is comparable to or larger than the frequency spread of the beam, Landau damping most likely will not rescue the beam from instability.

Consider the numerical example following Eq. (4.32) for the case of transverse rigid-beam instability due to the higher order rf cavity modes. The growth time without Landau damping was estimated to be 5 ms. To Landau damp this instability, the required frequency spread is roughly $\Delta\omega_\beta \approx \sqrt{3}/(5\text{ ms})$. This gives a required betatron tune spread of $\Delta\nu_\beta = 4 \times 10^{-5}$, which is rater small and is likely to be readily available. It is not too difficult to Landau damp this instability.

Exercise 5.10 Right on the stability boundary, the growth rate $\operatorname{Im}\Omega = 0$, but the mode frequency shift $\Delta\Omega = \operatorname{Re}\Omega - \omega_\beta \neq 0$. Show that

$$\frac{\Delta\Omega}{\Delta\omega} = \begin{cases} \dfrac{\operatorname{Re}\xi_1}{\Delta\omega}, & \text{Lorentz,} \\ \tanh\left(\dfrac{\Delta\omega}{|\xi_1|^2}\operatorname{Re}\xi_1\right), & \text{rectangular,} \\ \operatorname{sgn}(\operatorname{Re}\xi_1)\sqrt{1 - \dfrac{4}{3\pi}\dfrac{\Delta\omega}{|\xi_1|^2}\operatorname{Im}\xi_1}, & \text{parabolic,} \\ \dfrac{\Delta\omega}{2|\xi_1|^2}\operatorname{Re}\xi_1, & \text{elliptical,} \\ \operatorname{sgn}(\operatorname{Re}\xi_1)\sqrt{\sqrt{\dfrac{2|\xi_1|^2}{\Delta\omega\operatorname{Im}\xi_1}} - 1}, & \text{bi-Lorentzian,} \\ \operatorname{sgn}(\operatorname{Re}\xi_1)\sqrt{-2\ln\left(\sqrt{\dfrac{2}{\pi}}\dfrac{\Delta\omega}{|\xi_1|^2}\operatorname{Im}\xi_1\right)}, & \text{Gaussian.} \end{cases} \tag{5.63}$$

Observe that Landau damping does not affect the mode frequency shift for the Lorentz spectrum, as evidence also by the real part of Eq. (5.59).

A similar analysis can also be performed for the longitudinal Robinson instability using a one-particle model. In pace of Eqs. (4.4–4.5), we have

$$z''(s) + \left(\frac{\omega_s}{c}\right)^2 z(s) = \frac{Nr_0\eta}{\gamma C}\sum_{k=1}^{\infty}[\langle z\rangle(s) - \langle z\rangle(s - kC)]W_0''(-kC)$$
$$= \frac{Nr_0\eta}{\gamma C}Be^{-i\Omega s/c}\mathscr{W}, \tag{5.64}$$

where we have introduced

$$\langle z\rangle(s) = Be^{-i\Omega s/c} \tag{5.65}$$

and

$$\begin{aligned}\mathscr{W} &= \sum_{k=1}^{\infty} (1 - e^{i\omega_s kT_0}) W_0''(-kC) \\ &= \frac{i}{C} \sum_{p=-\infty}^{\infty} \left[p\omega_0 Z_0^{\parallel}(p\omega_0) - (p\omega_0 + \omega_s) Z_0^{\parallel}(p\omega_0 + \omega_s) \right].\end{aligned} \tag{5.66}$$

Self-consistency then gives rise to a dispersion relation

$$\frac{Nr_0\eta\mathscr{W}c^2}{2\omega_s\gamma C\Delta\omega} = \frac{1}{f(u) + ig(u)}, \tag{5.67}$$

which can be written in a form identical to Eq. (5.57), except that the complex mode frequency shift in the absence of Landau damping is now given by Eqs. (4.9–4.10), i.e.,

$$\xi_1 = -\frac{Nr_0\eta\mathscr{W}c^2}{2\omega_s\gamma C}. \tag{5.68}$$

The analysis for the transverse case therefore carries over straightforwardly to the longitudinal case. In particular, the simplified stability criterion (5.62) reads, in the longitudinal case,

$$\begin{aligned}|\xi_1| &= \frac{Nr_0\eta c^2}{2\omega_s\gamma C^2} \left| \sum_{p=-\infty}^{\infty} \left[p\omega_0 Z_0^{\parallel}(p\omega_0) - (p\omega_0 + \omega_s) Z_0^{\parallel}(p\omega_0 + \omega_s) \right] \right| \\ &< \frac{1}{\sqrt{3}} \Delta\omega_{1/2},\end{aligned} \tag{5.69}$$

where $\Delta\omega_{1/2}$ refers to the spread of synchrotron frequency of the beam particles.

The conclusion that the longitudinal Landau damping behaves analogously to the transverse case, however, is valid only for *bunched* beams for which $\omega_s \neq 0$, and under the assumption that the mode frequency shift is smaller than ω_s. In case of unbunched beams, $\omega_s = 0$, the longitudinal analysis gives results very different from its transverse counterpart. This point will be explained in more detail in Section 5.4.

Taking the numerical example following Eqs. (4.21–4.22), but assuming the rf frequency is tuned to the unstable side, the Robinson instability growth time is 1.2 ms. To Landau damp this instability requires a synchrotron frequency spread of $\Delta\omega_s \approx \sqrt{3}/(1.2\text{ ms})$, which corresponds to a relative spread of $\Delta\omega_s/\omega_s \approx 1.5\%$.

Although the above analyses assume a one-particle beam, one may venture to apply the result to a two-particle instability. For example, one may conclude that, to substantially raise the strong head-tail instability threshold by Landau damping, it is necessary to have a betatron frequency spread that is comparable to the synchrotron frequency. This is not easy to do in practice, and the conclusion discourages an attempt to Landau damp the strong head-tail instability.

5.3 TRANSVERSE INSTABILITY OF UNBUNCHED BEAMS

The previous section addressed the Landau damping of bunched beams. In this and the next section, we will address the Landau damping of unbunched beams. Consider an unbunched beam circulating in an accelerator as sketched in Figure 5.6(a). Let the beam have a rigid uniform round cross section with radius a. Consider an infinitesimal transverse displacement of the beam that behaves in time as $\exp(-i\Omega t)$ and in angular coordinate as $\exp(ins/R)$, where the integer n is a mode index and $2\pi R$ is the accelerator circumference. Observed at a fixed location s, the beam oscillates with a frequency Ω. Observed at a fixed time t as a snapshot, the beam makes n oscillations around the accelerator circumference. As will be analyzed in this section, this perturbation induces a perturbing electromagnetic wake field; the field acts back on the beam, leading to a reduction of an enhancement of the initial beam perturbation, and the beam is stable or unstable accordingly.

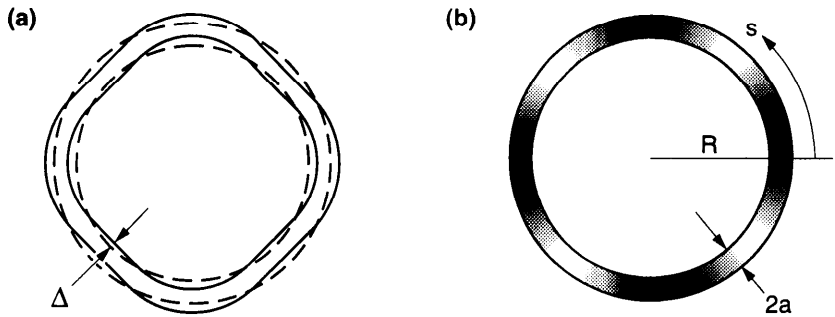

Figure 5.6. Snapshots of an unbunched beam executing a collective mode with mode index $n = 4$. (a) Transverse mode; dashed curves indicate the unperturbed beam. (b) Longitudinal mode; heavy and light shadings indicate the variation of the particle density distribution.

Now consider the beam in a vacuum chamber with a wake function $W_1(z)$ and a corresponding impedance $Z_1^{\perp}(\omega)$. The perturbing part of the oscillating beam has a ring-beam distribution

$$\rho = \frac{D}{\pi a^2}\delta(r - a)\cos\theta, \tag{5.70}$$

where D is the dipole moment per unit length; it is related to the maximum beam displacement Δ, shown in Figure 5.6(a), according to

$$D(s,t) = \frac{Ne\Delta}{2\pi R}\exp\left(in\frac{s}{R} - i\Omega t\right), \tag{5.71}$$

where N is the total number of particles in the beam.

The suggested dependence on t and s in Eq. (5.71) is an ansatz. It remains to be shown that this ansatz allows a self-consistent solution of the problem. Once established, Eq. (5.71) is remarkable in that it holds for an arbitrary impedance. An indication of its validity can be obtained by reviewing the multibunch analysis of Section 4.6. In particular, it is consistent with Eq. (4.127) on considering the limit $M \to \infty$ and identifying $\mu \to n$ and $n/M \to s/2\pi R$. Equation (4.127) is valid independent of the impedance, and so is Eq. (5.71).

The transverse force F_y on a test charge, at location s and time t, is determined by the dipole moment of the ring beam at the same location s as it past by at an earlier time t'. By superposition, the wake force is obtained by integrating the wake field over t'.[12] This gives

$$F_y(s,t) = -\frac{e}{2\pi R}\int_{-\infty}^{t} c\,dt'\,W_1(ct' - ct)\,D(s,t'). \tag{5.72}$$

Substituting Eq. (5.71) for D and expressing the result in terms of the impedance $Z_1^{\perp}$ yields

$$F_y(s,t) = ecD(s,t)i\frac{Z_1^{\perp}(\Omega)}{2\pi R}, \tag{5.73}$$

which is to be recognized as a rederivation of Eq. (2.70), since cD is just the dipole moment current. Note that the impedance is evaluated at frequency Ω. This is a consequence of the fact that it is responding to the beam signal observed at a fixed location. In particular, the impedance does not have any information on, and therefore does not respond to, the mode index n.

[12]Strictly speaking, a $\cos\theta$ ring beam generates a transverse wake force in the x-direction, but we will call it the y-direction.

Consider now a specific particle in the beam that passes position S at time 0. It is located at position $s = S + ct$ at time t, and experiences a transverse force $F_y(S + ct, t)$ at any time t. Modeling the impedance as evenly distributed around the accelerator circumference, the equation of motion of the particle is

$$\ddot{y} + \omega_\beta^2 y = \frac{F_y(S + ct, t)}{m_0 \gamma}$$
$$= \frac{N r_0 c^2}{\gamma T_0} i \frac{Z_1^\perp(\Omega)}{2\pi R} \Delta \exp\left[in \frac{S}{R} - i(\Omega - n\omega_0)t \right], \quad (5.74)$$

where we have defined the revolution frequency $\omega_0 = c/R = 2\pi/T_0$, and ω_β is the betatron frequency of the particle under consideration.

Although the impedance responds only to Ω, the moving particle sees a force with a driving frequency $\omega_d = \Omega - n\omega_0$. The solution of Eq. (5.74) with $s = S + ct$ for the particle under consideration, is

$$y(s, t) = \frac{N r_0 c^2}{\gamma T_0} i \frac{Z_1^\perp(\Omega)}{2\pi R} \frac{\Delta \exp[in(s/R) - i\Omega t]}{\omega_\beta^2 - (\Omega - n\omega_0)^2}. \quad (5.75)$$

Self-consistency requires that the beam at (s, t) have a displacement of $y(s, t) = \Delta \exp[in(s/R) - i\Omega t]$. This yields the dispersion relation

$$1 = \frac{N r_0 c^2}{\gamma T_0} i \frac{Z_1^\perp(\Omega)}{2\pi R} \frac{1}{\omega_\beta^2 - (\Omega - n\omega_0)^2}. \quad (5.76)$$

The mode frequency Ω is to be found from Eq. (5.76). The fact that the s and t dependences nicely cancel in obtaining Eq. (5.76) is a consequence of the correct choice of the ansatz (5.71).

There are two solutions of Eq. (5.76) for Ω, one close to $n\omega_0 - \omega_\beta$, the other close to $n\omega_0 + \omega_\beta$. In the following, we consider the solution close to $n\omega_0 + \omega_\beta$. The other solution would lead to an identical instability criterion. The solution to Eq. (5.76) can be written as

$$\Omega = n\omega_0 + \omega_\beta + \xi_1, \quad (5.77)$$

where

$$\xi_1 = -\frac{N r_0 c^2}{2\omega_\beta \gamma T_0} i \frac{Z_1^\perp(\Omega)}{2\pi R} \quad (5.78)$$

is the complex mode frequency shift in the absence of Landau damping.

In the unperturbd case, the mode frequency is given by $n\omega_0 + \omega_\beta$, and the beam displacement behaves according to $\exp[in(s - ct)/R - i\omega_\beta t]$. The beam displacement pattern rotates around the accelerator with an angular frequency $\omega_0 + (\omega_\beta/n)$. Waves with $n > 0$ are called *fast waves*; those with $n < 0$ are *slow waves*. The beam displacement observed at a fixed location s oscillates with frequency $n\omega_0 + \omega_\beta$. The displacement observed relative to the moving beam oscillates at frequency ω_β, as it should.

The quantity ξ_1 in Eq. (5.78) involves the impedance evaluated at frequency Ω, but to first order in beam intensity, it can be evaluated at the unperturbed frequency $n\omega_0 + \omega_\beta$. The instability growth rate is given by the imaginary part of Ω. According to Eq. (5.77), we have

$$\tau^{-1} = \operatorname{Im} \xi_1 = -\frac{Nr_0c^2}{2\omega_\beta\gamma T_0} \frac{\operatorname{Re} Z_1^\perp(n\omega_0 + \omega_\beta)}{2\pi R}. \tag{5.79}$$

Similarly, the mode frequency shift is given by

$$\Delta\Omega = \operatorname{Re} \xi_1 = \frac{Nr_0c^2}{2\omega_\beta\gamma T_0} \frac{\operatorname{Im} Z_1^\perp(n\omega_0 + \omega_\beta)}{2\pi R}. \tag{5.80}$$

Only the real part of the impedance appears in the growth rate, and only the imaginary part appears in the mode frequency shift.

It is interesting to note that Eq. (5.79) gives the same growth rate (4.28) obtained for a one-particle model of bunched beams if we add a summation over n in the expression. A similar summation of Eq. (5.80) over n gives Eq. (4.27) if the shift is interpreted as a shift in ω_β.

As an example, the resistive-wall impedance, Eq. (2.76), gives

$$\xi_1 = -\frac{Nr_0c^2}{\omega_\beta\gamma T_0 b^3} \frac{1}{\sqrt{2\pi\sigma|n\omega_0 + \omega_\beta|}} \left[1 + i \operatorname{sgn}(n\omega_0 + \omega_\beta)\right]. \tag{5.81}$$

The dominating mode occurs when n is equal to the nearest integer to $-\omega_\beta/\omega_0$. Let the betatron tune $\nu_\beta = \omega_\beta/\omega_0$ be written as $N_\beta + \Delta_\beta$, where Δ_β is the fractional part of ν_β, which can be positive or negative depending on whether ν_β is above or below its nearest integer N_β. The dominating mode is then a slow wave with $n = -N_\beta$. The instability growth rate and mode frequency shift are given by the imaginary and real parts of

$$\Omega - \Delta_\beta\omega_0 = -\frac{Nr_0c^2}{\omega_\beta\gamma T_0 b^3} \frac{1 + i \operatorname{sgn}(\Delta_\beta)}{\sqrt{2\pi\sigma\omega_0|\Delta_\beta|}}. \tag{5.82}$$

The growth rate agrees with Eqs. (4.33–4.34) if we keep the leading term $p = 0$ in the function $f(\Delta_\beta)$. The beam is stable if the tune is above an integer and unstable below an integer. Note that the frequency of this dominating mode is approximately $\Delta_\beta \omega_0$, which is usually much less than the betatron frequency ω_β. In obtaining Eq. (5.82) we have assumed the resistive wall is much thicker than the skin depth evaluated at frequency $\Delta_\beta \omega_0$.

So far we have not included Landau damping. In case not all particles have the same natural betatron frequency, and the beam has a spectrum $\rho(\omega)$ [normalized by $\int d\omega\, \rho(\omega) = 1$], the dispersion relation (5.76) reads

$$1 = \frac{Nr_0c^2}{\gamma T_0} i \frac{Z_1^\perp(\Omega)}{2\pi R} \int d\omega \frac{\rho(\omega)}{\omega^2 - (\Omega - n\omega_0)^2}. \tag{5.83}$$

There are two poles located at $\omega = \pm(n\omega_0 - \Omega)$. For a given mode n, usually only one of the pole terms dominates. Consider the $\omega = -n\omega_0 + \Omega$ pole. The dispersion relation can be written as

$$1 = -\xi_1 \int d\omega \frac{\rho(\omega)}{\omega - \omega_d}, \tag{5.84}$$

where $\omega_d = \Omega - n\omega_0$ is the frequency of the driving wake force and ξ_1 is given by Eq. (5.78).

Equation (5.84) assumes the dominance of a single pole, which follows if the mode frequency shift and growth rate are small compared with the natural focusing frequency ω_β (modulus ω_0) > 0. A similar assumption cannot be made in the case of longitudinal instability of unbunched beams because there is no natural focusing. As we will see in Section 5.4, this leads to a qualitatively different behavior of the longitudinal instability of unbunched beams.

To determine the instability threshold conditions, we have seen that Eq. (5.84) is to be interpreted as [see Eqs. (5.38) and (5.45)]

$$1 = -\xi_1 \left[\text{P.V.} \int d\omega \frac{\rho(\omega)}{\omega - |\omega_d|} + i\pi \operatorname{sgn}(\omega_d) \rho(|\omega_d|) \right] \tag{5.85}$$

or, using Eq. (5.27),

$$1 = -\frac{\xi_1}{\Delta\omega} [f(u) + ig(u)]. \tag{5.86}$$

The spectrum width $\Delta\omega$ and the functions $f(u)$ and $g(u)$ in Eq. (5.86) are as defined in the previous section, but ξ_1 is to be inserted from Eq. (5.78), and $u = (\omega_\beta - |\omega_d|)/\Delta\omega$. We have used in Eq. (5.86) the fact that $\omega_d > 0$ for the pole chosen because $\omega_d = \Omega - n\omega_0 \approx \omega_\beta > 0$. Had we chosen the other

pole with $\omega_d \approx -\omega_\beta$, we have to take the sign properly according to Eq. (5.85).

For a given spectrum, Eq. (5.86) gives the stability threshold condition. Beam stability is determined by whether the quantity $-\xi_1/\Delta\omega$ lies in the stable region in the complex $\mathscr{D}_1 = (f + ig)^{-1}$ plane, as shown in Figure 5.5. When unstable, the beam is said to have a *transverse microwave instability*, since the frequency $n\omega_0 + \omega_\beta$ of the beam signal observed by a pickup electrode is often in the microwave range.

The transverse instabilities of unbunched beams in the presence of Landau damping therefore follow closely those of the bunched beams. For example, a Lorentz spectrum gives the complex mode frequency

$$\Omega = n\omega_0 + \omega_\beta + \xi_1 - i\,\Delta\omega. \tag{5.87}$$

The beam stability condition is then

$$\text{Im}\,\xi_1 = -\frac{Nr_0c^2}{2\omega_\beta\gamma T_0}\frac{\text{Re}\,Z_1^\perp(n\omega_0 + \omega_\beta)}{2\pi R} < \Delta\omega. \tag{5.88}$$

One concludes from Eq. (5.88) the expected result that the frequency spread helps stabilize the beam.

The condition (5.88) is always satisfied if $\text{Re}\,Z_1^\perp(n\omega_0 + \omega_\beta) > 0$. It follows from Eq. (2.106) that fast waves are always stable. It is the stability of the slow waves that requires Landau damping.

In the case of a resistive wall, Eq. (5.88) gives the stability condition, for a beam with Lorentz spectrum,

$$-\frac{Nr_0c^2}{\omega_\beta\gamma T_0 b^3}\frac{\text{sgn}(\Delta_\beta)}{\sqrt{2\pi\sigma\omega_0|\Delta_\beta|}} < \Delta\omega, \tag{5.89}$$

where the left hand side is the growth rate without Landau damping and is given by the imaginary part of Eq. (5.82). For the beam to be stable against resistive-wall instability, we must choose the betatron tune to be either above an integer, i.e., $\Delta_\beta > 0$, or below an integer with

$$\Delta_\beta < -\left(\frac{Nr_0c^2}{\omega_\beta\gamma T_0 b^3\,\Delta\omega}\right)^2\frac{1}{2\pi\sigma\omega_0}. \tag{5.90}$$

Continuing the numerical example following Eqs. (4.34–4.35), we find the beam is unstable only in a very small tune region $0 > \Delta_\beta > -0.00013$ if there is a small betatron tune spread of $\Delta\omega/\omega_\beta = 10^{-6}$. Resistive-wall instability therefore does not noticeably affect the choice of betatron tunes in this example.

In case the detailed spectral distribution is not available, one could apply the simplified criterion (5.62), which now reads

$$|\xi_1| = \frac{Nr_0 c}{2\omega_\beta \gamma T_0^2} \left| Z_1^\perp (n\omega_0 + \omega_\beta) \right| < \frac{1}{\sqrt{3}} \Delta\omega_{1/2}. \tag{5.91}$$

It is interesting to note that Eq. (5.91) for the transverse stability of an unbunched beam gives, up to a numerical factor of the order of unity, the stability condition (4.46) for a bunched beam against the strong head-tail instability when one makes the replacement $\Delta\omega_{1/2} \to \omega_s$, identifies $|iZ_1^\perp/T_0|$ with W_0, and lets N be the number of particles in the bunch. This again supports the observation that synchrotron oscillation has a stabilizing effect against collective instabilities, and ω_s plays for bunched beams a role similar to the one the frequency spread $\Delta\omega_{1/2}$ plays for unbunched beams.

Landau damping results from a finite $\Delta\omega_{1/2}$, which is a spread of $n\omega_0 + \omega_\beta$. One source of this spread is an energy spread of the particles in the beam, which in fact gives two contributions: one due to the dependence of ω_β on δ through the chromaticity ξ, and the other due to a dependence of the revolution frequency ω_0 on δ through the slippage factor η. This leads to

$$\Delta\omega_{1/2} = | - n\omega_0 \eta + \xi\omega_\beta | \, \Delta\delta_{1/2}. \tag{5.92}$$

Inserting Eq. (5.92) into Eq. (5.91) gives a stability condition

$$\left| Z_1^\perp (n\omega_0 + \omega_\beta) \right| < Z_0 \frac{2\pi R\gamma | - n\eta + \xi\nu_\beta |}{\sqrt{3}\, Nr_0 \beta_Z} \Delta\delta_{1/2}, \tag{5.93}$$

where $Z_0 = 4\pi/c = 377\ \Omega$, and we have written ω_β/ω_0 as ν_β, the betatron tune, and c/ω_β as β_Z, the β-function at the location of the impedance.

In case $\xi = 0$, Landau damping comes from a spread in the revolution frequency due to energy spread. In case $\eta = 0$ (the beam is operated at transition), Landau damping comes from the chromaticity effect. For the particular mode which has $-n\eta + \xi\nu_\beta \approx 0$, Landau damping has to be provided by nonchromatic sources such as a spread in ω_β introduced by octupole magnets. To avoid this requirement, it would be desirable to arrange the parameters so that the condition $-n\eta + \xi\nu_\beta = 0$ occurs in the fast wave regime, where, as mentioned before, the mode is naturally damped.[13] This means $n > 0$, and ξ must have the same sign as η. In other words, it would be desirable to have $\xi > 0$ above transition and $\xi < 0$ below transition. This criterion is the same as that for a bunched beam against the

[13] J. Gareyte, *Frontiers of Particle Beams: Intensity Limitations*, Hilton Head Island, Lectures in Phys. **400**, Spring-Verlag, 1990, p. 14.

head-tail instability. There will be more discussion of this point when we come to Eqs. (6.264–6.265). Below we consider the case $\xi = 0$.

The stability criterion (5.93) has a few useful variations which are given below.

(i) For a broad band impedance, one may take $n\omega_0 + \omega_\beta$ to be approximately given by a certain cutoff frequency ω_c (most likely, $\omega_c \approx c/b$, where b is the vacuum chamber pipe radius), and $n \approx \omega_c/\omega_0$. Equation (5.93) becomes

$$|Z_1^\perp(\omega_c)| < Z_0 \frac{2\pi R\gamma|\eta|\omega_c}{\sqrt{3}\, N r_0 \beta_Z \omega_0} \Delta\delta_{1/2}. \tag{5.94}$$

(ii) In case the instability growth rate is much faster than the synchrotron oscillation, one may obtain a stability criterion against transverse microwave instability for *bunched* beams.[14] This is done by simply replacing the unperturbed beam density of an unbunched beam by the peak beam density of a bunched beam because, in the fast growing regime, the instability occurs locally and it would be the peak beam density that determines the instability threshold. For an elliptical distribution, this means replacing $N/2\pi R$ by $\sqrt{3}\, N_B/\pi\, \Delta z_{1/2}$, where N_B is the number of particles in the beam bunch. One then obtains from Eq. (5.94),

$$|Z_1^\perp(\omega_c)| < Z_0 \frac{\pi\gamma|\eta|\omega_c}{3N_B r_0 \beta_Z \omega_0} \Delta\delta_{1/2}\, \Delta z_{1/2}. \tag{5.95}$$

Equation (5.95) can also take another form if we note that

$$\Delta\delta_{1/2} = \frac{\omega_s}{|\eta|c} \Delta z_{1/2}. \tag{5.96}$$

We then have

$$|Z_1^\perp(\omega_c)| < Z_0 \frac{\pi\gamma\omega_s\omega_c}{3N_B r_0 \beta_Z \omega_0 c} \Delta z_{1/2}^2. \tag{5.97}$$

(iii) For a long bunch, the cutoff is not due to the pipe radius b, but due to the bunch length $\Delta z_{1/2}$. The cutoff frequency is given by $\omega_c \approx c/\Delta z_{1/2}$. Equation (5.97) then reads

$$|Z_1^\perp| < Z_0 \frac{\pi\gamma\omega_s}{3N_\beta r_0 \beta_Z \omega_0} \Delta z_{1/2}. \tag{5.98}$$

[14] D. Boussard, CERN Lab II/RF/Int 75-2 (1975); R. D. Ruth and J. M. Wang, IEEE Trans. Nucl. Sci. **NS-28**, 2405 (1981). This is called the *Boussard criterion* in the literature.

It may be instructive to consider another view of Eq. (5.98) as follows. Consider a bunch executing a transverse betatron oscillation. Its transverse wake force perturbs the betatron focusing force that is equivalent to a quadrupole magnet with field gradient $K \approx e\hat{I}Z_1^{\perp}/2\pi RE$, where E is the particle energy and $\hat{I} \approx N_B ec/\Delta z_{1/2}$ is the peak beam current. Beam stability requires that the wake induced betatron tune shift to be less than the synchrotron tune ω_s/ω_0 (recall the mechanism of the strong head-tail effect), i.e.,

$$\left|\frac{1}{2}\beta_Z RK\right| < \frac{\omega_s}{\omega_0}. \tag{5.99}$$

Equation (5.98) then follows.

Equations (5.94–5.98) apply to the transverse microwave instability. It is derived for unbunched beams, but has been extended heuristically to bunched beams. What Eq. (5.99) demonstrates is that the mechanism of the microwave instability is basically the same as that of the strong head-tail instability, which is also called the mode coupling instability in the literature.

We now have two simplified stability criteria for the transverse instability of bunched beams. One of them is Eq. (5.98), which applies when the instability growth rate $\gg \omega_s$. The other is Eq. (5.62), which holds when the growth rate $\ll \omega_s$. On the other hand, observing $\Sigma_p |Z_1^{\perp}(p\omega_0 + \omega_\beta)| \approx (\omega_c/\omega_0)|Z_1^{\perp}(\omega_c)|$ with $\omega_c \approx c/\Delta z_{1/2}$, it is interesting to note that Eq. (5.62) becomes Eq. (5.98)—up to a numerical factor of the order of unity—if we replace the betatron frequency spread $\Delta\omega_{1/2}$ by ω_s.

(iv) It is sometimes useful to relate the transverse impedance $|Z_1^{\perp}|$ to the longitudinal impedance $|Z_0^{\parallel}/n|$ by the approximate relation (2.108) even though the case being considered is for the transverse instability. For an unbunched beam, Eq. (5.94) gives

$$\left|\frac{Z_0^{\parallel}}{n}\right| < Z_0 \frac{\pi R\gamma|\eta|b}{\sqrt{3}\, Nr_0\beta_Z}\, \Delta\delta_{1/2}, \tag{5.100}$$

where we have assumed $\omega_c \approx c/b$. For a bunched beam, if the bunch length $\Delta z_{1/2}$ is shorter than the pipe radius b, Eqs. (5.95) and (5.97) give

$$\begin{aligned}\left|\frac{Z_0^{\parallel}}{n}\right| &< Z_0 \frac{\pi\gamma|\eta|b}{6N_B r_0\beta_Z}\, \Delta\delta_{1/2}\, \Delta z_{1/2} \\ &= Z_0 \frac{\pi\gamma\omega_s b}{6N_B r_0\beta_Z c}\, \Delta z_{1/2}^2.\end{aligned} \tag{5.101}$$

For a long bunch with $\Delta z_{1/2} > b$, the cutoff frequency is taken to be $\omega_c \approx c/\Delta z_{1/2}$, we have

$$\left|\frac{Z_0^{\parallel}}{n}\right| < Z_0 \frac{\pi\gamma|\eta|b^2}{6N_B r_0 \beta_Z} \Delta\delta_{1/2}$$

$$= Z_0 \frac{\pi\gamma\omega_s b^2}{6N_B r_0 \beta_Z c} \Delta z_{1/2}. \tag{5.102}$$

5.4 LONGITUDINAL INSTABILITY OF UNBUNCHED BEAMS

We have investigated the Landau damping effect for bunched beams—both the transverse and longitudinal cases—in Section 5.2. We have also investigated the transverse case for unbunched beams in Section 5.3. The analyses of these cases are all rather similar. In this section, the remaining case, the longitudinal case for unbunched beams, is treated. We will see that the analysis becomes quite different because there is no external focusing, i.e., $\omega_s = 0$. In particular, Landau damping in this case does not come directly from a spread in the natural focusing frequencies, but indirectly from a spread in the revolution frequencies.

Consider a relativistic unbunched beam executing a longitudinal collective motion as sketched in Figure 5.6(b). Let the unperturbed beam have a uniform distribution with the longitudinal line density

$$\lambda_0 = \frac{N}{2\pi R}. \tag{5.103}$$

Let the perturbation be an infinitesimal longitudinal density wave given by

$$\Delta\lambda(s,t) = \Delta\hat{\lambda} \exp\left(in\frac{s}{R} - i\Omega t\right). \tag{5.104}$$

The mode $n = 0$ is excluded because it violates charge conservation. The beam interacts with the vacuum chamber environment characterized by a longitudinal wake function $W_0'(z)$ and a corresponding impedance $Z_0^{\parallel}(\omega)$.

Consider a test charge at position s and time t. The longitudinal wake force F_s on the test charge is determined by the beam density as it passes by position s at an earlier time $t' < t$. By superposition, we have

$$F_s(s,t) = -\frac{e^2}{2\pi R}\int_{-\infty}^{t} c\,dt'\, W_0'(ct' - ct)\,\Delta\lambda(s,t'). \tag{5.105}$$

Substituting Eq. (5.104) for $\Delta\lambda$ and Eq. (2.72) for W_0' gives

$$F_s(s,t) = -e^2 c\,\Delta\lambda(s,t)\,\frac{Z_0^{\parallel}(\Omega)}{2\pi R}. \tag{5.106}$$

The last expression is to be compared with Eq. (2.64), identifying $ec\,\Delta\lambda$ as the instantaneous beam current.

Consider now a specific particle that passes position S at time $t = 0$. It experiences a longitudinal force $F_s(S + ct, t)$ at time t. Let the energy deviation and longitudinal coordinate of this particle be designated at δ_S and z_S; the equations of motion are

$$\begin{aligned} \dot{z}_S &= -\eta c \delta_S, \\ \dot{\delta}_S &= -\frac{r_0 c}{\gamma T_0}\,\Delta\hat{\lambda}\exp\left[in\frac{S}{R} - i(\Omega - n\omega_0)t\right] Z_0^{\parallel}(\Omega). \end{aligned} \tag{5.107}$$

We first ignore Landau damping. The solution to Eq. (5.107) is

$$\begin{aligned} \delta_S(t) &= -i\frac{r_0 c}{\gamma T_0}\,\frac{\Delta\hat{\lambda}}{\Omega - n\omega_0}\exp\left[in\frac{S}{R} - i(\Omega - n\omega_0)t\right] Z_0^{\parallel}(\Omega), \\ z_S(t) &= -\frac{nr_0 c^2}{\gamma T_0}\,\frac{\Delta\hat{\lambda}}{(\Omega - n\omega_0)^2}\exp\left[in\frac{S}{R} - i(\Omega - n\omega_0)t\right] Z_0^{\parallel}(\Omega). \end{aligned} \tag{5.108}$$

The density perturbation $\Delta\lambda$ is related to $z_S(t)$ by the equation of continuity. The particles in the space between s and $s + \Delta s$ in the unperturbed beam at time t are the same ones occupying the space between $s + z_{s-ct}(t)$ and $s + \Delta s + z_{s+\Delta s-ct}(t)$ at time t in the perturbed beam, so that their number is

$$\lambda_0\,\Delta s = [\lambda_0 + \Delta\lambda(s,t)]\{[s + \Delta s + z_{s+\Delta s-ct}(t)] - [s + z_{s-ct}(t)]\}, \tag{5.109}$$

which gives, for small Δs,

$$\begin{aligned} \Delta\lambda(s,t) &= -\lambda_0\frac{\partial z_{s-ct}}{\partial s} \\ &= \frac{2\pi N r_0 \eta}{\gamma T_0^3}\,\frac{in}{(\Omega - n\omega_0)^2}\,\Delta\hat{\lambda}\exp\left(in\frac{s}{R} - i\Omega t\right) Z_0^{\parallel}(\Omega). \end{aligned} \tag{5.110}$$

Self-consistency requires that the beam at (s, t) have a density perturbation of $\Delta\hat{\lambda}\exp(ins/R - i\Omega t)$. This yields the dispersion relation

$$1 = \frac{\xi_2}{(\Omega - n\omega_0)^2}, \tag{5.111}$$

where we have introduced a parameter

$$\xi_2 = i\frac{2\pi N r_0 n\eta}{\gamma T_0^3} Z_0^{\parallel}(n\omega_0). \tag{5.112}$$

To first order of perturbation, the impedance in Eq. (5.112) has been evaluated at the unperturbed frequency $n\omega_0$.

The real and imaginary parts of $\Omega - n\omega_0$ obtained from Eq. (5.111) give

$$\begin{aligned}\Delta\Omega = \mathrm{Re}(\Omega - n\omega_0) &= \mp \mathrm{sgn}(\mathrm{Im}\,\xi_2)\sqrt{\frac{|\xi_2| + \mathrm{Re}\,\xi_2}{2}} \\ &= \mp \mathrm{sgn}(n\eta)\sqrt{\frac{\pi N r_0}{\gamma T_0^3}\left(|n\eta Z_0^{\parallel}| - n\eta\,\mathrm{Im}\,Z_0^{\parallel}\right)}\end{aligned} \tag{5.113}$$

and

$$\begin{aligned}\tau^{-1} = \mathrm{Im}(\Omega - n\omega_0) &= \mp\sqrt{\frac{|\xi_2| - \mathrm{Re}\,\xi_2}{2}} \\ &= \mp\sqrt{\frac{\pi N r_0}{\gamma T_0^3}\left(|n\eta Z_0^{\parallel}| + n\eta\,\mathrm{Im}\,Z_0^{\parallel}\right)},\end{aligned} \tag{5.114}$$

where the impedance $Z_0^{\parallel}$ is evaluated at $n\omega_0$, and the $\pm$ signs refer to two solutions for the mode.

Recall that, in the transverse case, only the real part of the impedance appears in the growth rate and only the imaginary part appears in the mode frequency shift; this is no longer true here. For stability, τ^{-1} must not be positive for both solutions in Eq. (5.114). This is possible only when ξ_2 is real and positive, in which case the instability growth rate is zero. Away from the positive real axis, the + mode grows and the − mode damps.

The dispersion relation (5.111) has an important difference from the previous dispersion relations, namely, it is the *square* of the complex mode frequency shift $\Omega - n\omega_0$ that is related to the impedance here, whereas in all previous cases, the mode frequency shift is linearly related to the impedance.

This feature can be traced back to the fact that there is no external focusing in the longitudinal motion of an unbunched beam. This quadratic dependence has an important consequence. In all previous cases, half of the complex ξ_1-plane is stable even without Landau damping [see Figure 5.5(a)], whereas in the present case, as just mentioned [also see Figure 5.8(a) below], the corresponding stable region is restricted to the positive real ξ_2-axis. Landau damping is absolutely required against the longitudinal collective instabilities for unbunched beams. Once more one observes that synchrotron oscillation is one effective way to counteract collective instabilities.

Comparing Figure 5.8 with Figure 5.5, the quadratic nature of Eq. (5.111) is reflected in that the unstable (shaded) region of Figure 5.8 can be obtained from Figure 5.5 by a process of "folding over" its upper half plane. To illustrate this, consider Figure 5.5 and imagine rotating the negative real axis clockwise around the origin toward the positive real axis, stretching elastically the unstable region behind it; the process would result in a figure that resembles Figure 5.8. In the case without Landau damping, the only stable region after folding is the positive real axis. This folding operation—the equivalent of squaring a quantity in the complex plane—is applicable even in the presence of Landau damping for the various spectra illustrated.

Equation (5.111) can be compared with Eq. (4.8) obtained from a one-particle bunched beam. By dropping the potential-well distortion term and setting $\omega_s = 0$, Eq. (4.8) can be obtained by summing Eq. (5.111) over n from $-\infty$ to ∞.

As mentioned, the only chance of stability at this point is when Im $\xi_2 = 0$, i.e., when the impedance is purely imaginary. Furthermore, the impedance must be purely inductive above transition, and purely capacitance below transition.[15] Consider the case of the space charge effect, which is purely capacitive. Substituting the impedance Eq. (2.80) into Eqs. (5.113–5.114) gives

$$\Delta\Omega = \begin{cases} 0 & \text{if} \quad \eta > 0, \\ \pm \operatorname{sgn}(n) \sqrt{-\dfrac{Nr_0 n^2 c^2 \eta}{2\pi\gamma^3 R^3}\left(2\ln\dfrac{b}{a}+1\right)} & \text{if} \quad \eta < 0, \end{cases}$$

$$\tau^{-1} = \begin{cases} \mp \sqrt{\dfrac{Nr_0 n^2 c^2 \eta}{2\pi\gamma^3 R^3}\left(2\ln\dfrac{b}{a}+1\right)} & \text{if} \quad \eta > 0, \\ 0 & \text{if} \quad \eta < 0. \end{cases} \tag{5.115}$$

The beam is therefore longitudinally unstable above transition. This is in contrast with the bunched beam case, where the space charge force causes

[15]Recall that we call an impedance inductive or capacitive according to whether Im $Z_0^{\parallel}(\omega) < 0$ or > 0, respectively, in the region $\omega > 0$.

only a mode frequency shift and not an instability. This instability is called the *negative mass instability*.[16]

The physical origin of the negative mass instability can be illustrated as follows. Consider an unbunched beam, and let there be a small accidental density clustering at a certain position along the beam. The head and the tail of the cluster will experience space charge forces that push them apart in such a way that the head will be accelerated while the tail will be decelerated. The head therefore gains energy and the tail loses energy due to the space charge force. Above transition, one has the peculiar feature that a particle slows down if it gains energy because of the larger circumference it has to make—the longitudinal mass is negative. Therefore, the head of the cluster will move backward toward the center, and similarly, the tail of the cluster will move forward, also toward the center. The result is that the cluster becomes more clustered, creating a spontaneous lumping of the beam, leading to the negative mass instability above transition.

The fact that the unbunched beam is intrinsically unstable longitudinally in the absence of Landau damping is also reflected in the fact that $\tau^{-1} \propto |n|$ in Eq. (5.115). Physically, this is because the space charge force is proportional to the derivative $\lambda'(s)$ of the longitudinal beam density, which is in turn proportional to n. As a consequence, the beam becomes infinitely unstable with increasing mode number n. It is not meaningful to discuss longitudinal instability of unbunched beams without Landau damping.

Landau damping for the longitudinal instabilities of an unbunched beam comes from a spread in the revolution frequency ω_0 (which could result from an energy spread of the beam). Let $\rho(\omega_0)$ be the spectrum centered around $\bar{\omega}_0$ and satisfying $\int d\omega_0\, \rho(\omega_0) = 1$; then we have the dispersion relation

$$1 = \xi_2 \int d\omega_0 \frac{\rho(\omega_0)}{(n\omega_0 - \Omega - i\epsilon)^2} \tag{5.116}$$

where the impedance in the expression for ξ_2, Eq. (5.112), is to be evaluated at $n\bar{\omega}_0$. We have also attached an infinitesimal imaginary part to Ω according to the prescription (5.43). Given $\rho(\omega_0)$ and the impedance, Eq. (5.116) can be solved for the mode frequency Ω.

Exercise 5.11 Equation (5.115) shows that the beam is stable against the space charge effect below transition ($\eta < 0$) even if $\rho(\omega_0) = \delta(\omega_0 - \bar{\omega}_0)$, i.e., without Landau damping. What happens if $\rho(\omega_0)$ contains two δ-function peaks, $\rho(\omega_0) = \frac{1}{2}\delta(\omega_0 - \omega_a) + \frac{1}{2}\delta(\omega_0 - \omega_b)$ where $\omega_a \approx \omega_b \approx \bar{\omega}_0$?

[16]C. E. Nielson and A. M. Sessler, Rev. Sci. Instr. **30**, 80 (1959); C. E. Nielson, A. M. Sessler, and K. R. Symon, *Proc. Int. Conf. High Energy Accel. and Instru.*, CERN, 1959, p. 239; L. J. Laslett, V. K. Neil, and A. M. Sessler, Rev. Sci., Instr. **32**, 276 (1961); M. Q. Barton and C. E. Nielson, *Proc. Int. Conf. High Energy Accel.*, BNL, 1961, p. 16; H Bruck et al., *Proc. Int. Conf. High Energy Accel.*, BNL, 1961, p. 175.

Naively, one would expect the two-peak beam is more stable than a one-peak beam because it has a better chance of being Landau damped, but this is not so.

(a) Show that the beam becomes unstable due to space charge effect even below transition if ω_a and ω_b are sufficiently close to each other,

$$|\omega_a - \omega_b| < \sqrt{-\frac{4Nr_0\eta c^2}{\pi\gamma^3 R^3}\left(\ln\frac{b}{a} + \frac{1}{2}\right)}. \tag{5.117}$$

This instability is related to the *two-stream instability* in plasma physics.[17] Its mechanism involves the interplay and exchange of energies in the two beam streams.

(b) Establish the stability boundary diagram for the two-peak spectrum as will be done in Figure 5.8 for other spectra.

An integration by parts gives an alternative expression of Eq. (5.116),

$$\begin{aligned} 1 &= \frac{\xi_2}{n}\int d\omega_0 \frac{\rho'(\omega_0)}{n\omega_0 - \Omega - i\epsilon} \\ &= \frac{\xi_2}{n}\left[\text{P.V.}\int d\omega_0 \frac{\rho'(\omega_0)}{n\omega_0 - \Omega} + \frac{i\pi}{|n|}\rho'\left(\frac{\Omega}{n}\right)\right]. \end{aligned} \tag{5.118}$$

The absence of external focusing gives rise to the fact that Eq. (5.116) has a double pole, which in turn has the consequence that longitudinal Landau damping of unbunched beams involves the derivative of $\rho(\omega_0)$, as expressed in Eq. (5.118).

Denoting the spectrum width by $\Delta\omega$, the dispersion relation (5.118) can be written as

$$\frac{\xi_2}{n^2\Delta\omega^2} = \frac{1}{f(u) + i\,\text{sgn}(n)g(u)} \equiv \mathscr{D}_2, \tag{5.119}$$

where $u = (n\bar{\omega}_0 - \Omega)/(n\,\Delta\omega)$ and we have introduced

$$\begin{aligned} f(u) &= n\,\Delta\omega^2\,\text{P.V.}\int d\omega_0 \frac{\rho'(\omega_0)}{n\omega_0 - \Omega}, \\ g(u) &= \pi\,\Delta\omega^2\rho'\left(\frac{\Omega}{n}\right). \end{aligned} \tag{5.120}$$

[17]See for example Francis F. Chen, *Introduction to Plasma Physics*, Plenum Press, New York, 1977; Stanley Humphries, Jr., *Charged Particle Beams*, Wiley, New York, 1990.

Note that the functions f and g introduced here are different from those of Eq. (5.27). Equation (5.120) applies to the special case without external focusing.

For a δ-function spectrum (no Landau damping), we have

$$f = \frac{1}{u^2} \quad \text{and} \quad g = 0. \tag{5.121}$$

For a Lorentz spectrum (5.21), we have

$$f = \frac{u^2 - 1}{(u^2 + 1)^2} \quad \text{and} \quad g = \frac{2u}{(u^2 + 1)^2}. \tag{5.122}$$

For a rectangular spectrum Eq. (5.30), we have

$$f(u) = \frac{1}{u^2 - 1} \quad \text{and} \quad g(u) = \frac{\pi}{2}[\delta(u - 1) - \delta(u + 1)]. \tag{5.123}$$

For a tri-elliptical spectrum[18]

$$\rho(v) = \frac{8}{3\pi\,\Delta\omega}(1 - v^2)^{3/2} H(1 - |v|), \qquad v = \frac{\bar{\omega}_0 - \omega_0}{\Delta\omega}, \tag{5.124}$$

with $H(x)$ the step function, we have

$$\begin{aligned} f &= -4\left[1 - 2u^2 + 2|u|\sqrt{u^2 - 1}\, H(|u| - 1)\right], \\ g &= 8u\sqrt{1 - u^2}\, H(1 - |u|). \end{aligned} \tag{5.125}$$

For a parabolic spectrum (5.32), we have

$$\begin{aligned} f &= -3\left[1 - \frac{u}{2} \ln\left|\frac{u + 1}{u - 1}\right|\right], \\ g &= \frac{3\pi}{2} u H(1 - |u|). \end{aligned} \tag{5.126}$$

For a bi-Lorentzian spectrum (5.34), we have

$$f = \frac{u^4 + 6u^2 - 3}{(u^2 + 1)^3} \quad \text{and} \quad g = \frac{8u}{(u^2 + 1)^3}. \tag{5.127}$$

Figure 5.7 exhibits the functions $f(u)$ and $g(u)$ for the various spectra. The function f resembles, but is not identical to, the second derivative ρ''.

[18]The tri-elliptical spectrum was not one of the examples mentioned in Eqs. (5.28–5.35). The reason for introducing it here will become clear when we reach Eq. (5.130).

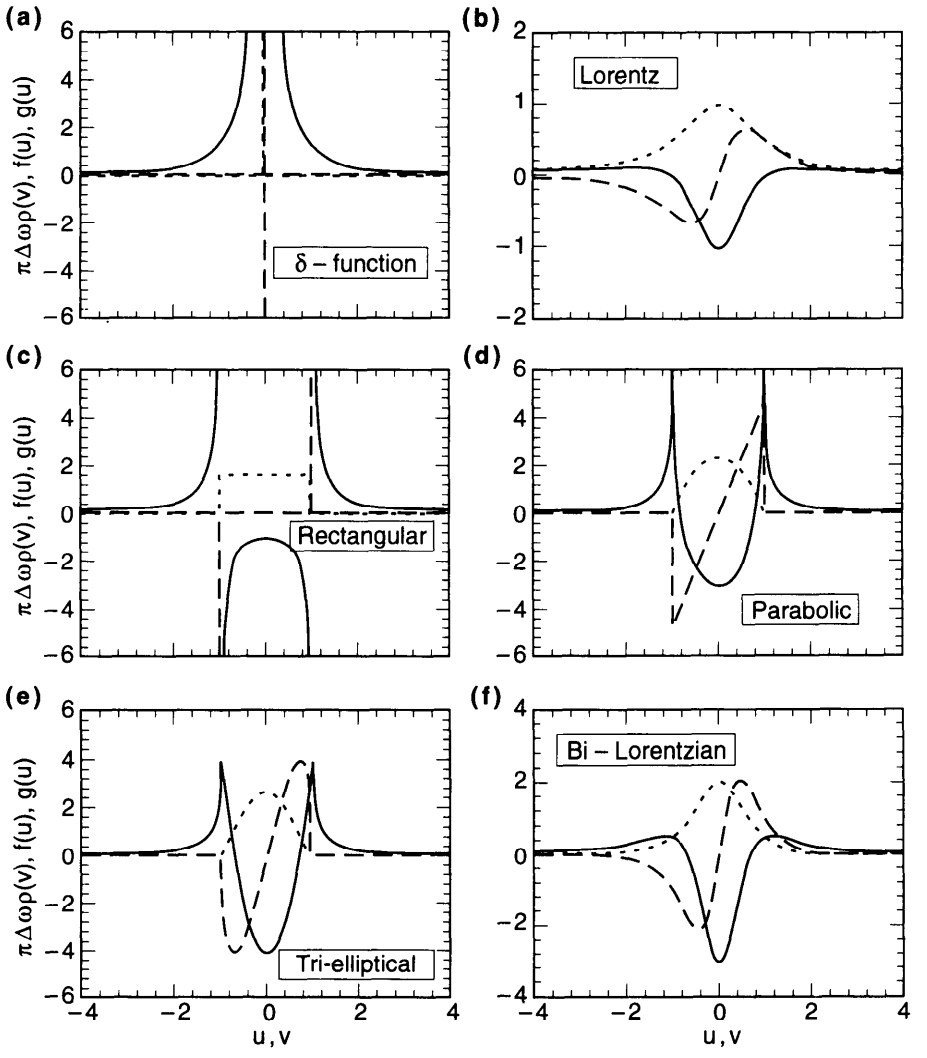

Figure 5.7. Functions $f(u)$ (solid curves) and $g(u)$ (dashed curves) of Eq. (5.120) for various spectra of revolution frequencies. Dotted curves are for $\pi\,\Delta\omega\,\rho(v)$. The function g is proportional to ρ' and the function f resembles $-g' \propto \rho''$.

The case of Lorentz spectrum is particularly simple. The mode frequency shift is the same as the case without Landau damping, Eq. (5.113), except that the impedance is to be evaluated at $n\bar{\omega}_0$. The growth rate is given by

$$\tau^{-1} = \mp\sqrt{\frac{\pi N r_0}{\gamma T_0^3}\left(|n\eta Z_0^{\parallel}| + n\eta\ \mathrm{Im}\ Z_0^{\parallel}\right)} - |n|\,\Delta\omega. \qquad (5.128)$$

Compared with Eq. (5.114), Eq. (5.128) contains an extra term $-|n|\,\Delta\omega$, which is always negative, demonstrating a damping effect. Note that the damping term, unlike its transverse counterpart Eq. (5.87), is proportional to the mode index n. The higher the mode index, therefore, the more strongly the mode is Landau damped. This behavior is expected because the disturbance $\Delta\hat{\lambda}\, e^{-ins/R}$ in beam density distribution disperses faster for higher mode index n due to a spread $\Delta\omega$ of the revolution frequency.

To damp the negative mass instability with a Lorentz spectrum requires a spectral width

$$\frac{\Delta\omega}{\bar{\omega}_0} > \sqrt{\frac{Nr_0\eta}{2\pi\gamma^3 R}\left(2\ln\frac{b}{a}+1\right)} \qquad (\eta > 0). \tag{5.129}$$

Take for example a proton accelerator with $R = 150$ m, $N = 2\times 10^{12}$, $\gamma = 10$, $\eta = 0.01$, $b = 10$ cm, and $a = 5$ mm; the required spread of revolution frequency is $\Delta\omega/\bar{\omega}_0 = 0.5\times 10^{-6}$. If this spread is to come from an energy spread, the required energy spread is $\Delta\delta = \Delta\omega/|\eta|\bar{\omega}_0 = 0.5\times 10^{-4}$.

For a general spectrum, the procedure following Eqs. (5.57–5.58) can also be applied here to obtain the stability boundary diagrams. Figure 5.8 shows the lotus of $\mathscr{D}_2$ of Eq. (5.119) as the parameter u is scanned from $-\infty$ to ∞ in the complex $\mathscr{D}_2$-plane. The beam is unstable if the value of $\xi_2/(n^2\,\Delta\omega^2)$ lies in the shaded region. Case (a) in Figure 5.8 is without Landau damping; the stability region is only along the positive real axis. This is not much improved with the rectangular spectrum in case (c). The stability region is extended to $(-1, 0)$, but stays confined to the real axis. The most stable case is offered by the Lorentz spectrum (b); the stability region is inside a parabolic boundary. Case (d), for a parabolic spectrum, gives a stable region which is cherry-shaped (complete with a stem). Case (e), for the tri-elliptical spectrum, gives a circular stable region (a lollipop). In the unstable region, the unbunched beam is said to have a *longitudinal microwave instability*.

If one does not have detailed spectral information and is interested in a rough estimate whether the beam is stable against the longitudinal microwave instability, a simplified stability criterion can be used,[19]

$$|\xi_2| = \frac{2\pi Nr_0}{\gamma T_0^3}\left|n\eta Z_0^{\parallel}(n\omega_0)\right| < \frac{1}{4}n^2\,\Delta\omega^2, \tag{5.130}$$

where the factor $\frac{1}{4}$ is such that the condition is exact for the tri-elliptical spectrum. An analogous treatment for the transverse microwave instability was given in Eq. (5.91).

[19]E. Keil and W. Schnell, CERN Report TH-RF/69-48 (1969); V. K. Neil and A. M. Sessler, Rev. Sci. Instr. **36**, 429 (1965). This is sometimes referred to as the *Keil-Schnell criterion* in the literature.

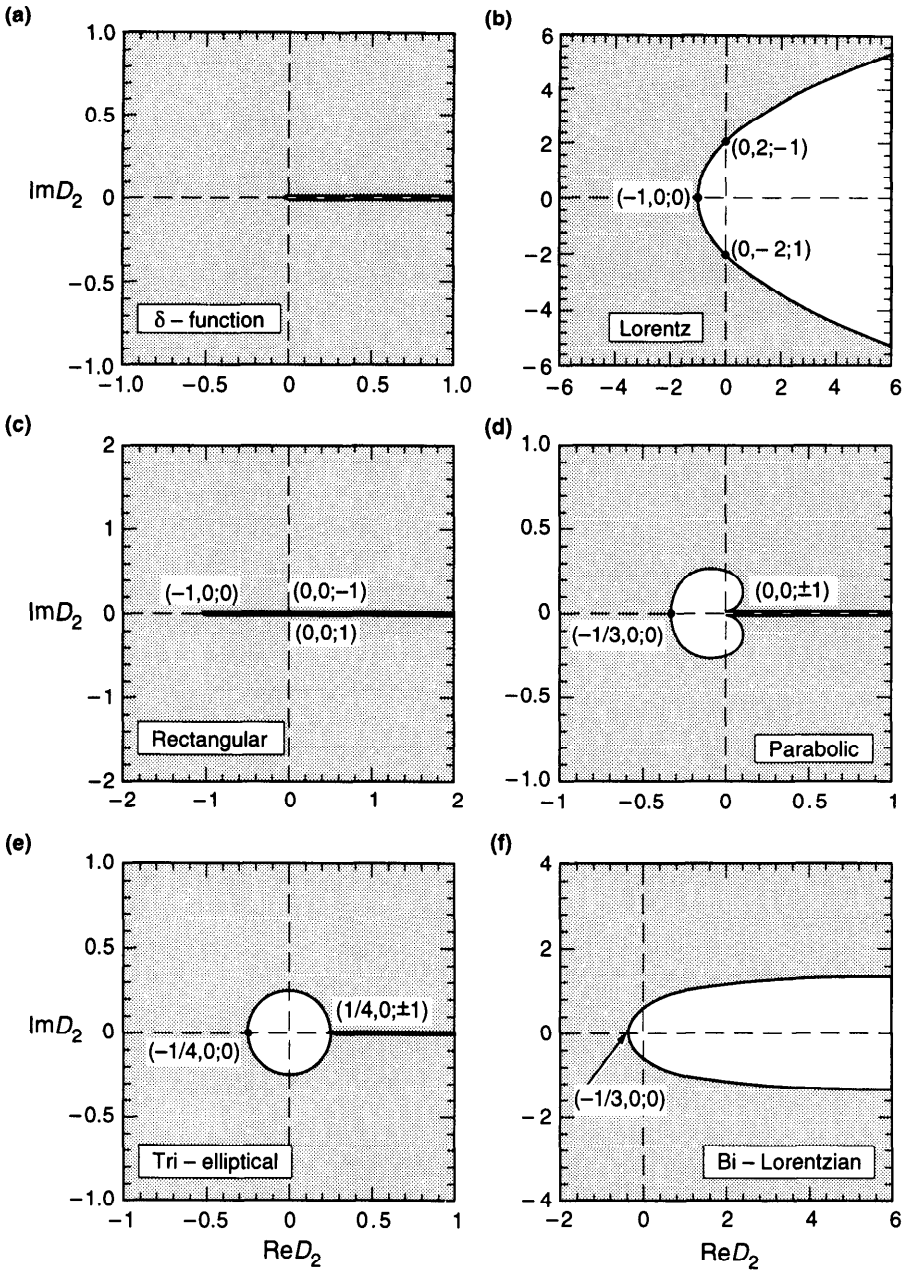

Figure 5.8. Stability boundary diagrams for various spectra in the complex $\mathscr{D}_2$-plane. If the complex quantity $\xi_2 / (n^2 \Delta\omega^2)$ lies in a shaded region, the beam is unstable. The numbers in parentheses are (Re $\mathscr{D}_2$, Im $\mathscr{D}_2$; sgn$(n)u$).

Relating $\Delta\omega$ to the half width at half maximum for the tri-elliptical distribution, we rewrite Eq. (5.130) as

$$|\xi_2| < \frac{1}{4}n^2\frac{\Delta\omega_{1/2}^2}{1-\left(\frac{1}{2}\right)^{2/3}} = 0.68n^2\,\Delta\omega_{1/2}^2. \tag{5.131}$$

If the spread in revolution frequency ω_0 comes from the energy spread of the beam, we must consider, to be consistent, also a tri-elliptical distribution for δ with

$$\Delta\omega_{1/2} = \bar{\omega}_0|\eta|\,\Delta\delta_{1/2}. \tag{5.132}$$

We then obtain from Eq. (5.131) the stability condition

$$\left|\frac{Z_0^{\parallel}(n\bar{\omega}_0)}{n}\right| < 0.68Z_0\frac{\pi|\eta|\gamma R}{Nr_0}\,\Delta\delta_{1/2}^2, \tag{5.133}$$

where $Z_0 = 377\ \Omega$.

Observe that, instead of imposing a condition on the impedance $Z_0^{\parallel}$ directly, Eq. (5.133) imposes a stability condition on $Z_0^{\parallel}/n$. In the present context, the quantity $Z_0^{\parallel}/n$ is a consequence of balancing the instability strength $|\xi_2|$, which is proportional to $nZ_0^{\parallel}$, and the Landau damping effect, which is proportional to $n^2\,\Delta\omega^2$. [See Eq. (5.130).] One may take another viewpoint, that the final stability condition should involve not the impedance but the impedance per unit length. By identifying $N/2\pi R$ on the right hand side of Eq. (5.133) as the line density of the beam, and recognizing that $Z_0^{\parallel}/n$ has the meaning of the impedance per unit length, one may anticipate the form of Eq. (5.133).

For a resistive-wall impedance, the worst mode is the one with the smallest n, i.e., $n = \pm 1$ (the mode $n = 0$ is excluded by charge conservation). The stability condition is given by

$$\Delta\delta_{1/2}^2 > \frac{Nr_0}{0.68|\eta|\gamma T_0 b\sqrt{\pi\sigma\bar{\omega}_0}}. \tag{5.134}$$

Resuming the numerical example following Eq. (5.129), and taking $\sigma = 3 \times 10^{17}\ \text{s}^{-1}$ for aluminum, the required beam energy spread is about 1×10^{-5}, a condition easily fulfilled.

In the case of a bunched beam, if the microwave instability growth rate is much faster than the synchrotron oscillation frequency, one may apply the Boussard criterion and modify Eq. (5.133) as was done in Eq. (5.95) for the transverse microwave instability. This is accomplished by replacing the unperturbed uniform density $N/2\pi R$ by the peak density across the length of the

bunch.[20] For a tri-elliptical distribution, it is replaced by $0.516N_B/\Delta z_{1/2}$, where N_B is the number of particles in the beam bunch. The resulting stability criterion for a bunched beam against longitudinal microwave instability reads

$$\left|\frac{Z_0^{\parallel}(n\bar{\omega}_0)}{n}\right| < 0.66Z_0\frac{|\eta|\gamma}{N_B r_0}\Delta\delta_{1/2}^2\,\Delta z_{1/2}. \tag{5.135}$$

If the impedance comes from a broad-band resonator, we have from Eq. (2.124) that $|Z_0^{\parallel}/n| \approx fZ_0/2$, where f is the effective fraction of the accelerator circumference occupied by deep cavities of size comparable to the vacuum chamber radius. Taking $\eta = 0.01$, $N_B = 10^{10}$, $\gamma = 10$, $\Delta\delta_{1/2} = 10^{-4}$, and $\Delta z_{1/2} = 0.1$ m, we find the stability condition $f < 1\%$.

An application of Eq. (5.96) gives an alternative form of Eq. (5.135),

$$\left|\frac{Z_0^{\parallel}(n\bar{\omega}_0)}{n}\right| < 0.66Z_0\frac{\omega_s^2\gamma}{|\eta|c^2N_B r_0}\Delta z_{1/2}^3. \tag{5.136}$$

Additional discussion of this can be found in connection with Eq. (6.160).

It may be instructive to sketch a more physical picture for the form of Eq. (5.136) as follows. Consider a bunch of length $\Delta z_{1/2}$. It induces a wake voltage $V \approx \hat{I}Z_0^{\parallel}$ where $\hat{I} \approx N_B ec/\Delta z_{1/2}$ is the peak beam current and $Z_0^{\parallel}$ is evaluated at the beam spectral frequency $\omega \approx c/\Delta z_{1/2} = n\omega_0$. Beam stability requires that V be less than the variation of the externally applied rf voltage across the bunch length, i.e.,

$$\left|\frac{1}{2\pi R}\frac{eV}{E}\right| < \left|\frac{1}{\eta}\left(\frac{\omega_s}{c}\right)^2\Delta z_{1/2}\right|. \tag{5.137}$$

Equation (5.136) follows from Eq. (5.137).

As in the transverse case [see discussion following Eq. (5.99)], we have two forms of the simplified stability criterion for the longitudinal instability of bunched beams: Eq. (5.136) when the growth rate $\gg \omega_s$, and Eq. (5.69) when the growth rate $\ll \omega_s$. Also as in the transverse case, these two forms are related to each other if one observes $|\Sigma_p(p\omega_0 + \omega_s)Z_0^{\parallel}(p\omega_0 + \omega_s)| \approx \omega_0(\omega_c/\omega_0)^3(Z_0^{\parallel}/n)$, where $\omega_c \approx c/\Delta z_{1/2}$, and if the synchrotron frequency spread $\Delta\omega_{1/2}$ is replaced by ω_s.

Comparing the microwave stability criteria of bunched beams in the transverse case, Eqs. (5.101–5.102), and the longitudinal case, Eq. (5.135), we

[20] D. Boussard, CERN Lab II/RF/Int 75-2 (1975); J. M. Wang and C. Pelligrini, *Proc. 11th Int. Conf. High Energy Accel.*, Geneva, 1980, p. 554.

conclude that the longitudinal microwave instability demands a more stringent stability condition if

$$\Delta\delta_{1/2} \lesssim 0.8\begin{cases} b/\beta_Z, & \text{short bunch,} \\ b^2/(\beta_Z \Delta z_{1/2}), & \text{long bunch.} \end{cases} \tag{5.138}$$

Since $\Delta\delta_{1/2}$ is proportional to $\Delta z_{1/2}$, it follows from Eq. (5.138) that the longitudinal instability is more stringent for short bunches. This feature should be evident from Figure 2.6.

For high energy applications, as the design energy of the accelerator increases, there is a tendency (for cost saving reasons) to reduce the vacuum chamber size b and increase the β-function. According to Eq. (5.138), this means the transverse microwave instability becomes increasingly more important relative to the longitudinal microwave instability unless the bunch length is reduced. To optimize the accelerator design, one may choose a short bunch with

$$\Delta\delta \approx 0.8b/\beta_Z$$

so that the transverse and the longitudinal instability limits are reached simultaneously.

5.5 BEAM TRANSFER FUNCTIONS

In practical accelerator operations, it is often useful to find out how the beam responds to a sinusoidal driving force. This beam response can be described in terms of a quantity called the *beam transfer function* (BTF), which is the subject of this section. The interest in the BTF is based on the fact that it contains a wealth of detailed information about the beam and the accelerator. The examination of the BTF constitutes a valuable diagnostic technique in operating an accelerator.[21]

When driven by an external sinusoidal force of frequency ω_d, the beam responds according to Eq. (5.36) with Ω replaced by ω_d. The result is conveniently summarized by the quantity $f(u) + ig(u)$, where $u = (\omega_x - \omega_d)/\Delta\omega$ with ω_x the central value of the beam frequency spectrum and $\Delta\omega$ the spectrum width. As we will soon see, the quantity $f + ig$ is the zero-intensity limit of the BTF.

When the driving frequency ω_d is far from ω_x, the BTF $f + ig$ is small and is almost purely real. This means the beam hardly responds, and the weak response $\langle x \rangle$ is either in phase or 180° out of phase relative to the

[21] H. Grunder and G. Lambertson, *Proc. 8th Int. Conf. High Energy Accel.*, CERN 1971, p. 308; A. Faltens, E. C. Hartwig, D. Möhl, and A. M. Sessler, *Proc. 8th Int. Conf. High Energy Accel.*, CERN, 1971, p. 338; A. Hofmann and B. Zotter, IEEE Trans. Nucl. Sci. **NS-24**, 1478 (1977); J. Borer et al., IEEE Trans. Nucl. Sci. **NS-26**, 3405 (1979); A. Hofmann, *Proc. 11th Int. Conf. High Energy Accel.*, Geneva, 1980, p. 540; J. Gareyte, *AIP Proc.* **184**, *Phys. Part. Accel.*, Fermilab 1987 and Cornell 1988, p. 343.

driving force depending on whether ω_x is above or below ω_d, respectively. When ω_d is close to ω_x, the BTF is almost purely imaginary with a large magnitude. This means the beam responds resonantly and $\langle x \rangle$ has a 90° phase relative to the driving force. This behavior can be seen from Figure 5.3, which shows the functions $f(u)$ and $g(u)$ for several spectral distributions. Figure 5.7 shows f and g for the special case when there is no external focusing.

We learned from the previous sections that the reciprocal of the BTF [for example, $\mathscr{D}_1$ in Eq. (5.58), $\mathscr{D}_2$ in Eq. (5.119)] plays a key role in the analysis of Landau damping. Figure 5.5 shows the lotus of $\mathscr{D}_1$ in the complex $\mathscr{D}_1$-plane as ω_d is scanned across the beam spectrum. The resulting diagram is the stability boundary diagram. Figure 5.8 shows similar results for $\mathscr{D}_2$.

The functions f and g, like the real and imaginary parts of an impedance, form Hilbert transforms pairs,[22]

$$f(u) = -\frac{1}{\pi}\text{P.V.}\int_{-\infty}^{\infty} du' \frac{g(u')}{u' - u},$$
$$g(u) = \frac{1}{\pi}\text{P.V.}\int_{-\infty}^{\infty} du' \frac{f(u')}{u' - u}. \tag{5.139}$$

The BTF $f + ig$ does not have singularities in the lower half of the complex u-plane. Its Fourier transform

$$G(t) = -\frac{i}{2\pi}\int_{-\infty}^{\infty} \frac{d\omega}{\Delta\omega}\left[f\left(\frac{\omega_x - \omega}{\Delta\omega}\right) + ig\left(\frac{\omega_x - \omega}{\Delta\omega}\right)\right]e^{-i\omega t} \tag{5.140}$$

satisfies the causality condition that $G(t) = 0$ if $t < 0$. In fact, $G(t)$ describes the beam response to a shock excitation (or to the initial conditions x_0 and $\dot{x}_0$) at time $t = 0$.

Exercise 5.12 With a Lorentz spectrum, (a) show that the BTF has only one pole at $u = i$; (b) verify the Hilbert transform property (5.139); (c) compute the Green's function $G(t)$; and (d) using Eq. (5.25), relate $G(t)$ to $\langle x \rangle / x_0$ when $\dot{x}_0 = 0$, and to $(1/\dot{x}_0)\, d\langle x \rangle / dt$ when $x_0 = 0$.

The BTF, or its reciprocal 1/BTF, can be determined experimentally by measuring the phase and amplitude of the beam response to an externally applied sinusoidal driving force. The information obtained gives detailed data about the beam frequency spectrum. In its simplest form, this is the routine method used to measure the central betatron tunes of circular accelerators.

[22]A. Hofmann, *Proc. CERN Accel. School*, Berlin, 1987, CERN Report 89-01 (1989), p. 40.

In a more sophisticated application, the detailed frequency spectrum can be related to the nonlinearities in the accelerator focusing system.

In addition, the BTF also provides a way to determine the impedance of the accelerator. To illustrate this, consider a one-particle bunched beam under the influence of a transverse impedance. Let the beam intensity be sufficiently low that the beam is stable against collective instabilities. When an external sinusoidal force is applied to the beam, the equation of motion is[23] [cf. Eq. (5.46)]

$$y''(s) + \left(\frac{\omega_\beta}{c}\right)^2 y(s) = -\frac{Nr_0}{\gamma C}\sum_{k=1}^{\infty}\langle y\rangle(s - kC)W_1(-kC) + \frac{A}{c^2}e^{-i\omega_d s/c}. \tag{5.141}$$

As a result of the driving force, the beam responds with the driving frequency. Let the beam response $\langle y\rangle$ be written as

$$\langle y\rangle(s) = Be^{-i\omega_d s/c}. \tag{5.142}$$

The right hand side of Eq. (5.141) then reads

$$\left(-\frac{Nr_0}{\gamma C}B\mathscr{W} + \frac{A}{c^2}\right)e^{-i\omega_d s/c}, \tag{5.143}$$

where $\mathscr{W}$ is given by Eqs. (5.49) or (5.50), but with the substitution $\omega_\beta \to \omega_d$.

Following an analysis similar to that for Landau damping, with Eq. (5.143) assuming the role of a driving force, allows us to write down the self-consistency condition

$$B = \left(-\frac{Nr_0\mathscr{W}c}{\gamma T_0}B + A\right)\frac{1}{2\omega_\beta\,\Delta\omega}[f(u) + ig(u)], \tag{5.144}$$

which can be solved for the beam transfer function, defined as

$$\begin{aligned}\text{BTF} &\equiv 2\omega_\beta\,\Delta\omega\,\frac{B}{A}\\ &= \frac{1}{\mathscr{D}_1(u) + \dfrac{\xi_1}{\Delta\omega}},\end{aligned} \tag{5.145}$$

[23]We have assumed both the impedance and the driving force are uniformly distributed around the accelerator circumference. Localized impedance and driving force complicate the analysis and are beyond the scope of the present treatment.

where $\mathscr{D}_1 = 1/(f + ig)$, and ξ_1 is the complex mode frequency shift (5.56) in the absence of Landau damping. A similar analysis for the longitudinal one-particle model leads to the same Eq. (5.145) with ξ_1 given by Eq. (5.68).

For low intensity beams, Eq. (5.145) gives BTF $= 1/\mathscr{D}_1 = f + ig$, as mentioned at the beginning of this section. Since $f(u)$ and $g(u)$ are intimately related to the beam spectral distribution, measurements of 1/BTF (or BTF) for a weak beam as ω_d scans across the beam spectrum yield detailed information on the spectral distribution. As the beam intensity increases, the measured 1/BTF contains additional information on $\mathscr{W}$, which in turn contains information on the impedance.

When the beam is stable against the collective instability, the BTF remains finite as ω_d is scanned across the beam spectrum. As the beam intensity gets closer to the instability threshold, the beam responds more strongly to the driving force, the BTF becomes larger, the lotus in the complex BTF plane moves away from the origin, and the 1/BTF lotus gets closer to—but does not cross—the origin in the complex 1/BTF plane. At the instability threshold (5.57), the denominator of the BTF (5.145) vanishes and the BTF diverges when ω_d reaches the value Ω of the collective mode frequency.

Exercise 5.13 Instead of driving the beam with a sinusoidal force, one could kick the beam at $t = 0$ and observe its subsequent response. Consider a beam behavior described by Eq. (5.54). Show that the beam response $\langle x \rangle(t)$ after the initial kick $x(0) = x_0$ and $\dot{x}(0) = \dot{x}_0$ satisfies the equation

$$\langle x \rangle(t) = x_0 \dot{G}(t) + \dot{x}_0 G(t) + \int_0^t dt' \, G(t - t') \left[W_1 \langle x \rangle(t') + \frac{W_2}{\omega_x} \frac{d}{dt'} \langle x \rangle(t') \right], \quad (5.146)$$

where

$$G(t > 0) = \int d\omega \, \rho(\omega) \frac{\sin \omega t}{\omega}. \quad (5.147)$$

Show that the solution of $\langle x \rangle$ in terms of the Fourier transformed quantities is

$$\langle \tilde{x} \rangle(\omega) = \frac{\tilde{G}(\omega)(-i\omega x_0 + \dot{x}_0)}{1 - 2\tilde{G}(\omega)\left(W_1 - i\dfrac{\omega}{\omega_x} W_2\right)}. \quad (5.148)$$

Specialize this to a Lorentz spectrum for a more concrete example. Make use of the result obtained in Exercise 5.12. Equation (5.146), the time-domain equivalent of the BTF, can be used as an experimental means to extract information on the wake function and the impedance.

For a bunched beam, the quantity ξ_1 is related to the impedance in a complicated manner according to Eqs. (5.50) and (5.66). For unbunched beams, the relation becomes simpler if we consider a driving force $\propto \exp(-i\omega_d t + ins/R)$ applied to a beam with zero chromaticity, causing it to execute a dipole motion with displacement $\Delta \exp(-i\omega_d t + ins/R)$. For a particle that passes location S at time $t = 0$, the equation of motion is [cf. Eq. (5.74)]

$$\ddot{y} + \omega_\beta^2 y = \left[\frac{Nr_0c^2}{\gamma T_0} i \frac{Z_1^\perp(\omega_d)}{2\pi R}\Delta + A\right] \exp\left[in\frac{S}{R} - i(\omega_d - n\omega_0)t\right]. \quad (5.149)$$

Following the now familiar procedure to solve Eq. (5.149) and demanding self-consistency, we obtain

$$\text{BTF} \equiv 2\omega_\beta \Delta\omega \frac{\Delta}{A} = \frac{1}{\mathscr{D}_1(u) + \xi_1/\Delta\omega}, \quad (5.150)$$

where $u = (\omega_\beta + n\omega_0 - \omega_d)/\Delta\omega$, and ξ_1 is given by Eq. (5.78) with the impedance evaluated at ω_d. For an unbunched beam, ξ_1 is therefore directly related to the impedance at the well-defined frequency ω_d. Having measured the 1/BTF with a weak beam to obtain $\mathscr{D}_1$, a measurement of an unbunched beam at modest intensity therefore yields direct information on the impedance.

Take a resonator impedance for example. We have

$$\frac{1}{\text{BTF}} = \frac{1}{f(u) + ig(u)} - i\frac{Nr_0c^2R_S\omega_R}{2\omega_\beta\gamma T_0^2\,\Delta\omega} \frac{1}{\omega_R\omega_d + iQ(\omega_R^2 - \omega_d^2)}. \quad (5.151)$$

If the resonator impedance is sufficiently broad that its width is larger than the width of $\omega_\beta + n\omega_0$ in the beam spectrum, the 1/BTF lotus is simply shifted by an amount proportional to $Z_1^\perp(\omega_\beta + n\omega_0)$. If the resonator width is smaller than the beam spectrum width, the 1/BTF lotus makes a loop when the driving frequency is scanned through the resonant frequency ω_R.

Figure 5.9 illustrates the behavior. The parameters used[24] are $\omega_R/\omega_0 = 200.1$, $Nr_0c^2R_S\omega_R/(8\pi^2\omega_\beta\gamma\,\Delta\omega) = 2 \times 10^4$, $\omega_\beta/\omega_0 = 6.094$, and a betatron tune spread of $\Delta\omega/\omega_0 = 0.005$. The most prominent mode under these conditions is a fast wave with $n = 194$. The resonance $\omega_d = \omega_R$ occurs slightly above ω_β and is within the spectrum width. Two cases are shown in Figure 5.9: one with $Q = 5 \times 10^5$, corresponding to a resonance whose width is narrower than the beam spectrum; the other with $Q = 2000$, having a resonance wider than the spectrum. Being a fast wave, the mode is necessarily stable. The same conclusion can be drawn by observing the fact that the

[24]These numbers are for illustration purpose only; they are not necessarily realistic.

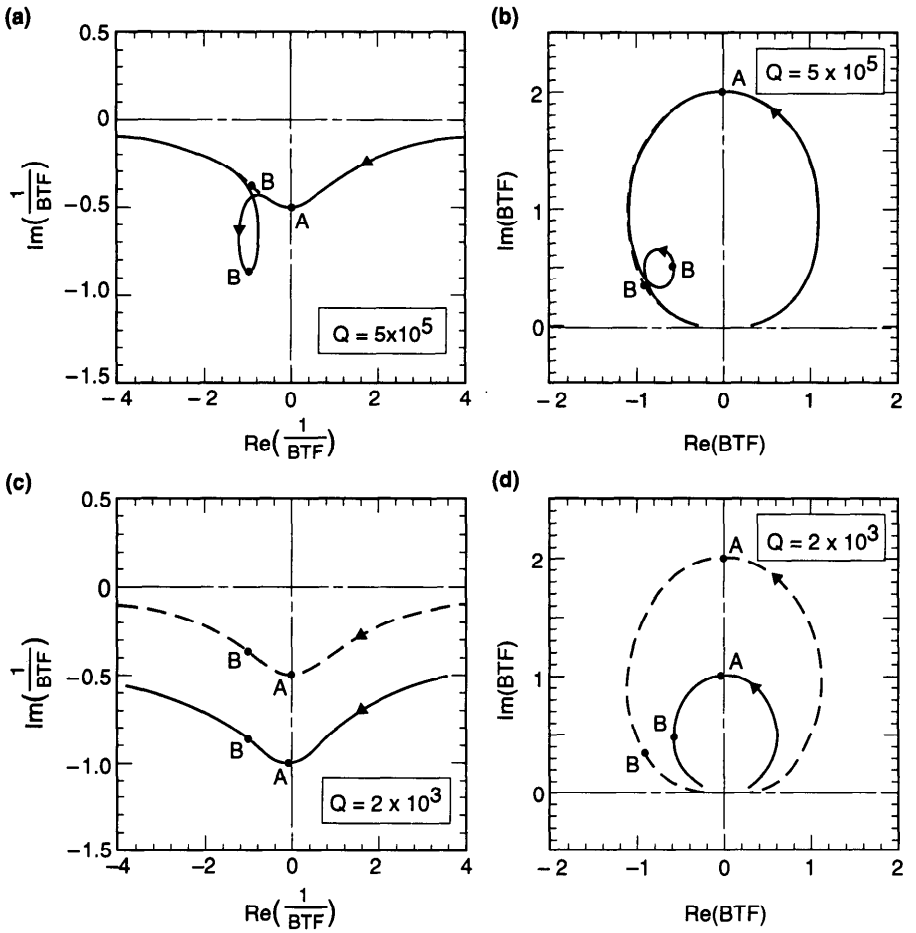

Figure 5.9. The beam transfer functions and their reciprocals trace out lotuses in their respective complex planes as the driving frequency is scanned across the beam spectrum. (a) 1/BTF for a resonator impedance whose width is sharper than the beam spectrum. (b) BTF for the impedance of case (a). (c) 1/BTF for a resonator impedance whose width is broader than the beam spectrum. (d) BTF for the impedance of case (c). A bi-Lorentzian spectrum has been assumed. The dashed curves are for the case of zero beam intensity. The dashed curves in (a) and (c) are reproductions of the stability boundary diagram shown in Figure 5.5(f). Arrows indicate the direction of the trace as ω_d sweeps through the beam spectrum from below. Locations marked by *A* and *B* are where ω_d is equal to $\omega_\beta - 6\omega_0$ and $\omega_R - 200\omega_0$, respectively.

resonant frequency ω_R is slightly above an integer times ω_0 and $\Delta_\beta > 0$, which assures beam stability according to Eq. (4.32). This is also reflected in the fact that the solid curves in Figure 5.9(b) and (d) stay on the inner side of the dashed curves. In case of Figure 5.9(c), the entire 1/BTF curve shifts by approximately a constant amount $\xi_1/\Delta\omega$, which for the case shown is almost purely imaginary.